



High-resolution geophysical data unravel the post-Variscan structural history of the NW Cotentin inner shelf (Central English Channel)

Tassadit Kaci^a, Bernard Le Gall^b, Anne Duperret^{a,*}, David Graindorge^b, Stephane Baize^c, Yann Méar^d

^a UMR 6294 LOMC, CNRS, Université Le Havre Normandie, Le Havre, France

^b UMR 6538 Geo-Ocean, Univ Brest, CNRS, Ifremer, F-29280 Plouzané, France

^c Institut de Radioprotection et Sécurité Nucléaire, Fontenay-aux-Roses, France

^d EA 4253 LUSAC, UNICAEN, CNAM-INTECHMER, Cherbourg-en-Cotentin, France

ARTICLE INFO

Editor: Michele Rebesco

Keywords:

NW offshore Cotentin peninsula
High-resolution geophysical records
Variscan inherited faults
Post-Eocene basin inversion and fault reactivation
Recent incision processes

ABSTRACT

The Cotentin Peninsula (CP) is one of the only area in Europe which contains records of a > 2.5 Ga-lasted geological history including three orogenic events (Archaean, Cadomian and Variscan) followed by a polyphase basin/inversion evolution during Meso-Cenozoic times. The CP area sensu lato is thus a suitable place for discussing how the structural configuration of the basement might have influenced the development of part of the southern shelf margin of the Central English Channel, even if sediments and post-Variscan tectonic records are limited at this place. This issue is addressed through an onshore/offshore structural approach combining newly-acquired high resolution bathymetric data and reflection seismic profiles, further constrained by lateral correlations onshore. The resulting Land-Sea Digital Elevation Model and corresponding geological map reveal a number of fault-bounded blocks involving a relatively thin package of Jurassic to Plio-Quaternary sequences, locally involved in slightly compressional deformations. These specific sedimentary and tectonic features typically characterize the southern shelf margin of the Central English Channel. They are discussed in terms of basin development and inversion processes in relation with basement structures and then integrated in the English Channel basin framework. Special attention is paid to three major structural features, i.e. the La Hague Offshore Fault, the La Hague Deep Fault network and the La Hague Deep, which emphasize, respectively, the role of structural inheritance and erosion/incision/deposition events during the post-Variscan tectono-sedimentary history of the southern elevated shoulder of the Central English Channel.

1. Introduction

In the framework of the European geological context, the Cotentin Peninsula (CP) provides the opportunity to address a > 2 Ga-lasted history which includes three orogenic events (Icartian, 2.2 to 1.8 Ga; Cadomian, 650 to 540 Ma and Variscan, 360 to 258 Ma) and the basal evolution recorded by most part of the English Channel in Meso-Cenozoic times (Fig. 1). The resulting structural pattern has benefited from numerous field tectonic studies principally focused on the Cadomian and Variscan belts (Chantraine et al., 1994; Dissler et al., 1988; Dissler and Gresselin, 1988; Dupret et al., 1990; Graindorge, 1998) and, to a lesser extent, on discrete Meso-Cenozoic basins (e.g. Carentan, Ecréhou in Fig. 2a) assumed to have been partly controlled by basement structures (Aubry, 1982; Pareyn and L'Homer, 1989; Ziegler, 1990;

Evans et al., 1990; Baize et al., 1998). But, due to the modest dimensions of these post-Variscan basins, which are further little exposed, very few was known about their structural evolution through time. That made difficult comparisons with the long-lasted and polyphase history recorded by the English Channel basins in Meso-Cenozoic times (e.g. Four-niguet, 1987; Ziegler, 1987a, 1987b; Bois et al., 1990a, 1990b; Ziegler et al., 1995; Lagarde et al., 2003; Le Roy et al., 2011).

In order to fill this gap, geophysical records have been performed in the NW offshore extent of the CP area where post-Variscan sedimentary deposits were previously mapped from sparse coring and dredging investigations (Lefort, 1975; Larssonneur et al., 1975; Bouysse et al., 1975). Our study is based on an onshore-offshore approach combining high-resolution bathymetric data (multibeam echosounder and LiDAR records) and high-resolution seismic reflection profiles, further calibrated

* Corresponding author.

E-mail address: anne.duperret@univ-lehavre.fr (A. Duperret).

<https://doi.org/10.1016/j.margeo.2024.107333>

Received 28 December 2023; Received in revised form 29 May 2024; Accepted 6 June 2024

Available online 7 June 2024

0025-3227/© 2024 Published by Elsevier B.V.

by a few offshore dated rock samples and then correlated with onshore geology. That leads us to elaborate a 17 × 23 km land-sea digital elevation model (DEM) and a corresponding geological map which both reveal first-order Meso-Cenozoic basin and fault structures. The spatio-temporal development of these post-Variscan basins is addressed in terms of structural inheritance during both their initiation and inversion stages. Comparisons are also attempted between the structural evolution of the NW offshore CP area on the shallow southern shelf margin of the English Channel and those recorded by extensive depositional areas in the central and western part of the English Channel. Lastly, the proposed tectonic scheme supplies new constraints for a seismotectonic revised framework in the CP area.

2. Geodynamic and onshore geological settings

2.1. Geodynamic setting

On a broad scale, the onshore/offshore CP area under study occurs on the southern shelf margin of the English Channel basinal framework, and more especially in the SE prolongation of the Cotentin Start Point ridge (Avedik, 1975), known as a NW-SE inherited Variscan structure which extends onshore in SW England along the Stickelpath-Lustleigh fault zone (SLF, Fig. 1). In the English Channel, the structural trends swing from SW-NE (Western Approaches and SW Channel basins) to E-W (Central Channel basin) on both sides of this transverse basement ridge. Given its elevated structural position, the CP shelf margin recorded an incomplete and more fragmented Meso-Cenozoic sedimentary (and tectonic) history than those in the long-lived and subsiding axial part of the English Channel. In the Western Approaches, extensional tectonics was principally accommodated by SW/NE-trending regional fault

structures in Upper Jurassic-Lower Cretaceous times (e.g. Alderney-Ushant Fault Zone (AUFZ) and Mid Channel Fault Zone (MCFZ) in Fig. 1; Ziegler et al., 1979; Bois et al., 1990b; Le Roy et al., 2011). In Southern England, the N-S/NE-SW extension is recorded in the Wessex, Weald-Artois and Central Channel basins by faulted half grabens facing predominantly to the north (Fig. 1) (Lake and Karner, 1987; Stoneley, 1992). Later on, some of these Meso-Cenozoic basins (e.g. Purbeck-Wight-Bray and Weald anticlines) recorded the effect of a N-S (then NW-SE) compression, in response to the Eurasia-Africa convergence (Whittaker, 1985; Lake and Karner, 1987; Mascle and Cazes, 1987; Ziegler, 1990; Hamblin et al., 1992; Chadwick, 1993; Ziegler et al., 1995; Guillocheau et al., 2000; Vandycke and Bergerat, 2001; Van Vliet-Lanoë et al., 2004). The basin inversion process in the Channel operated via successive pulses starting mainly at the end of Late Cretaceous (Laramide phase) (Ziegler, 1987c; Guillocheau et al., 2000; Vandycke and Bergerat, 2001; Vandycke, 2002; Van Vliet-Lanoë et al., 2004), followed by Cenozoic inversions from 40 to 39 Ma (Upper Eocene; Pyrenean phase) until ca. 24 Ma during the Late Oligocene Pyrenean and Alpine orogens (Bevan and Hancock, 1986; Ziegler, 1987c; Ziegler et al., 1995; Thimon et al., 2001). The Cenozoic compression also led to the reactivation of regional-scale N130°-150°E (Kerforne-type, KF in Fig. 1) and E-W/NE-SW fault systems (Vandycke, 2002; Raimbault et al., 2018). These compressive events alternated with relaxation phases and were also accompanied by regional-scale uplift of the Armorican Massif as a whole (Bonnet et al., 2000; Bessin et al., 2015).

2.2. Onshore geological setting

In contrast, the onshore geology in the CP area is dominated by the

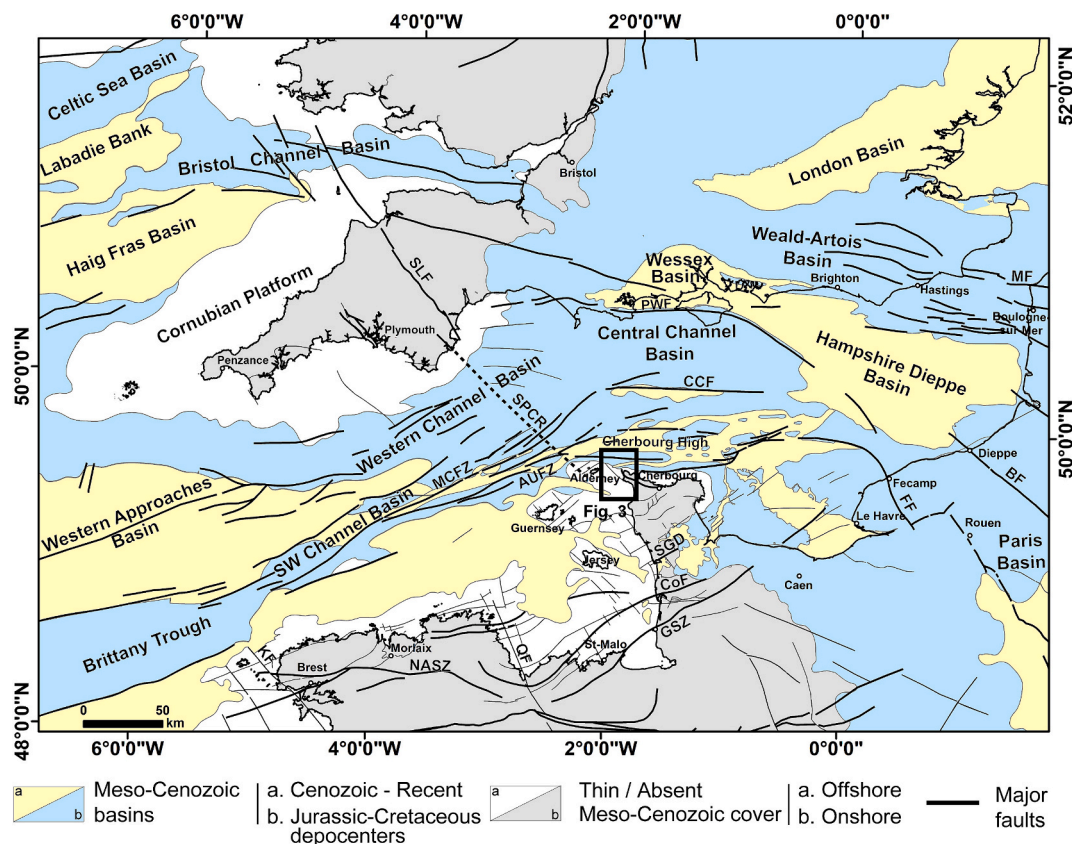


Fig. 1. Meso-Cenozoic basin configuration in the English Channel, simplified from Ziegler (1987a), Mortimore (2011), Duperré et al. (2012). AUFZ: Alderney-Ushant fault zone; BF: Bray fault; CCF: Central Channel fault; CoF: Coutances fault; FF: Fecamp fault; GSZ: Granville shear zone; KF: Kerforne fault; QF: Quessoy Nort-sur-Erdre fault; MCFZ: Mid Channel fault zone; MF: Midi fault; NASZ: North Armorican shear zone; PWF: Purbeck-Wight fault; SGD: Saint Germain discontinuity; SLF: Stickelpath-Lustleigh fault; SPCR: Start Point Cotentin ridge.

imprint of pre-Mesozoic structures, only little reworked in more recent times.

2.2.1. Icartian and Cadomian basement

Icartian series are dominated by ca 2.0 Ga-old metamorphic rocks extending along a NE-SW oriented belt from Guernsey to the CP (Fig. 2). In the CP studied area, they chiefly occur in the Jobourg cape (Auvray et al., 1979; Chantraine et al., 2001). Brioverian series include low-grade metamorphic volcanic and terrigenous rocks occurring south of the Coutances Fault (CoF) and in the northern hangingwall block of the North Cotentin Shear Zone (NCSZ, Figs. 2a, b) (Chantraine et al., 1994; Chantraine et al., 2001). The Cadomian deformation (650–540 Ma) is chiefly expressed by an ENE-WSW sinistral shear zone pattern including the Granville (GSZ) and Coutances (CoF) structures (Fig. 2a). The crustal geometry of Cadomian structures is imaged on SWAT and ARMOR deep

seismic reflection profiles as NW-dipping thrusts merging into a basal sole thrust at ~20 km depth, on top of the layered lower crust (Bois et al., 1991; Bitri et al., 2001). A last Cadomian event is marked by the intrusion of several granitoids (580, 573 and 515 Ma-old Gréville, Thiebot and Auderville granites) (Jonin and Vidal, 1975; Inglis et al., 2005) on both sides of the La Hague Cape (Fig. 2a, c).

2.2.2. Paleozoic series and Variscan deformation

The overlying Paleozoic metasedimentary series (Lower Cambrian up to Devonian, Fig. 2) were initially deposited in a large-scale basin encompassing the western part of the CP and most of the offshore Normano-Breton Gulf (NBG). At that stage, the Saint-Germain-sur-Ay discontinuity (SGD) behaved as a major basin bounding structure (Figs. 2a, b) (Le Gall et al., 2021). Carboniferous deposits were spatially restricted to the discrete Montmartin basin (Mo). The Variscan

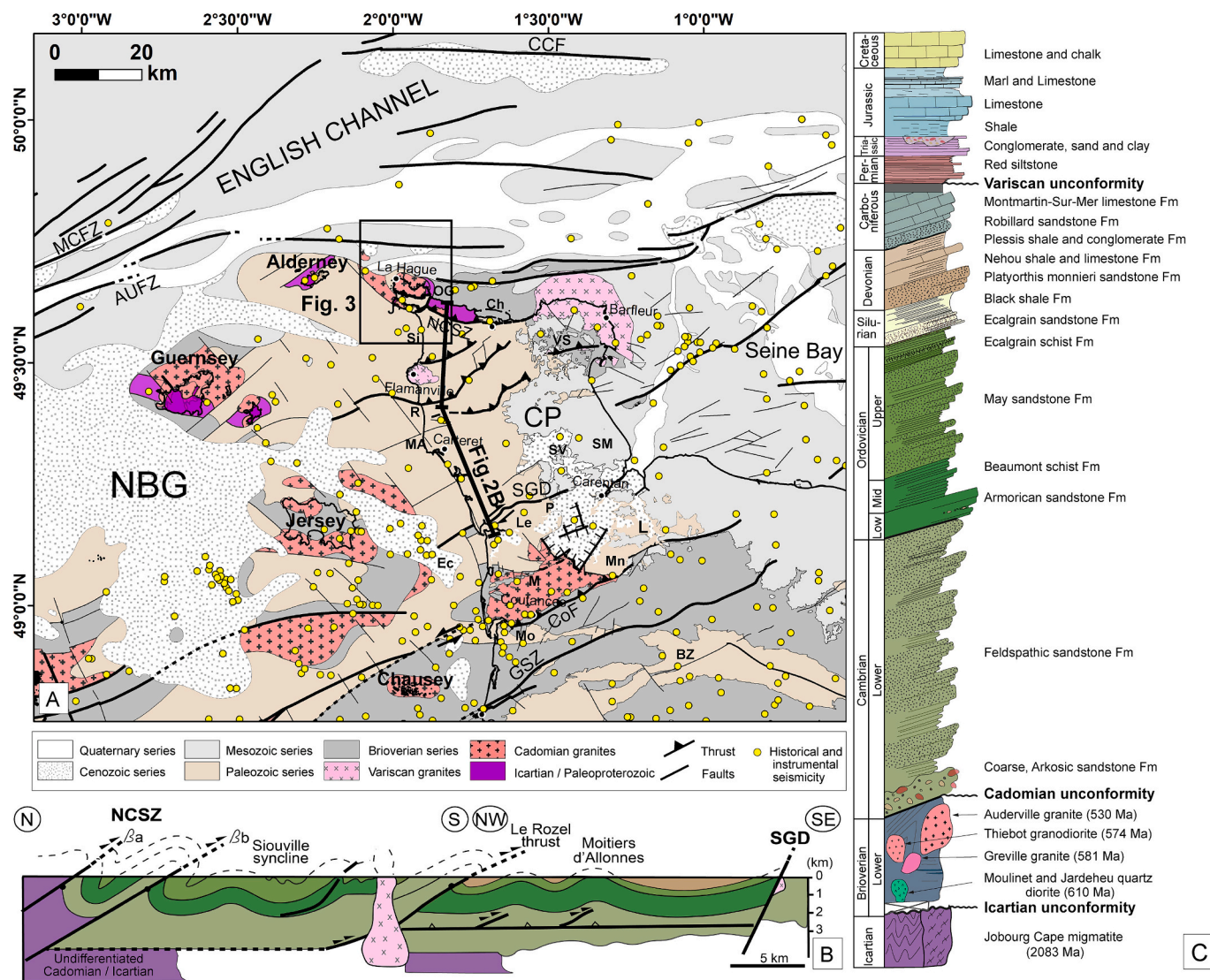


Fig. 2. Geological units in the onshore/offshore Cotentin peninsula (CP) area. (A) Simplified geological map of the Normano-Breton Gulf and the CP area, adapted from Chantraine et al. (2003) and Ballèvre et al. (2013). Yellow circles indicate epicentral location of the historical and instrumental seismicity. Historical seismicity is reported between 1091 and 1962 (SisFrance Catalog, www.sisfrance.net). Instrumental seismicity is shown from 1962 to 2023 (Cara et al., 2015) for 1962–2009 and the french unified catalog (LDG, BCSF-RéNaSS) for 2010–2023. AUFZ: Alderney Ushant fault zone. BZ: Bocaine zone, CCF: Central Channel fault, Ch: Cherbourg, CoF: Coutances fault, CP: Cotentin peninsula, Ec: Ecrehou basin, GSZ: Granville shear zone, J: Jobourg syncline, Le: Lessay basin, L: Littry basin, MA: Moitiers d'Allonnes anticline, MCFZ: Mid-Channel fault zone, Mn: Sainteny-Marchésieux, M: Montsurvent, Mo: Montmartin syncline, NBG: Normano-Breton gulf, NCSZ: North Cotentin shear zone, OG: Omonville-Gréville, P: Le Plessis basin, R: Rozel, Si: Siouville syncline, SGD: Saint-Germain-sur-Ay discontinuity, SM: Sainte-Mère-Eglise, SV: St-Sauveur-le-Vicomte basin, VS: Val-de-Saire. (B) Structural cross-section showing the tectonic style of the Variscan deformation in the North Cotentin fold-and-thrust belt, modified from Le Gall et al. (2021). (C) Lithostratigraphic column of the North Cotentin series, as established on the BRGM geological maps. (For interpretation of the references to colour in this figure legend, the reader is referred to the web version of this article.)

deformation resulted in a thin-skinned fold-and-thrust belt involving large wavelength folds (Siouville (Si) and Jobourg (Jo) synclines) and southerly-directed thrusts (NCSZ, Fig. 2b) (Dissler, 1987; Dissler et al., 1988; Dupret et al., 1990; Gresselin, 1990). Variscan strain dies out south of the SGD which thus likely acted as a fold/cleavage front (Le Gall et al., 2021). The CP basement area is thus partitioned into two contrasting domains involving: (i) a mobile Variscan belt to the north, superimposed on a previous Paleozoic (Ordovico/Devonian) basal domain and (ii) a stable domain to the south which encompasses the discrete and nearly unstrained Montmartin (Mo) Carboniferous basin and the moderately strained Bocaine Zone (BZ) (Le Gall et al., 2021).

The best evidence of Variscan overprint in the CP area are: (i) the reverse reactivation of Cadomian shear zones as thrusts (GSZ and CoF),

combined to a sinistral strike-slip component (CoF) (Doré et al., 1988) and (ii) the rejuvenation of the SGD as a dextral fault (Doré et al., 1988). These events occurred contemporaneously with the emplacement of the Flamanville and Barfleur granites (Fig. 2a) at 318 ± 1.5 Ma (U/Pb zircon; Martin et al., 2018).

2.2.3. Post-Variscan history

The first post-Variscan sedimentary series in the CP area were deposited in discrete Permo-Carboniferous limnic basins (Plessis (P) and Molay-Littry (L); Fig. 2a). Their Mesozoic history is not documented because of missing geological records. During Cenozoic times, the CP and surrounding areas were subject to intense weathering and erosion, whereas coastal deposits accumulated in several small basins in the

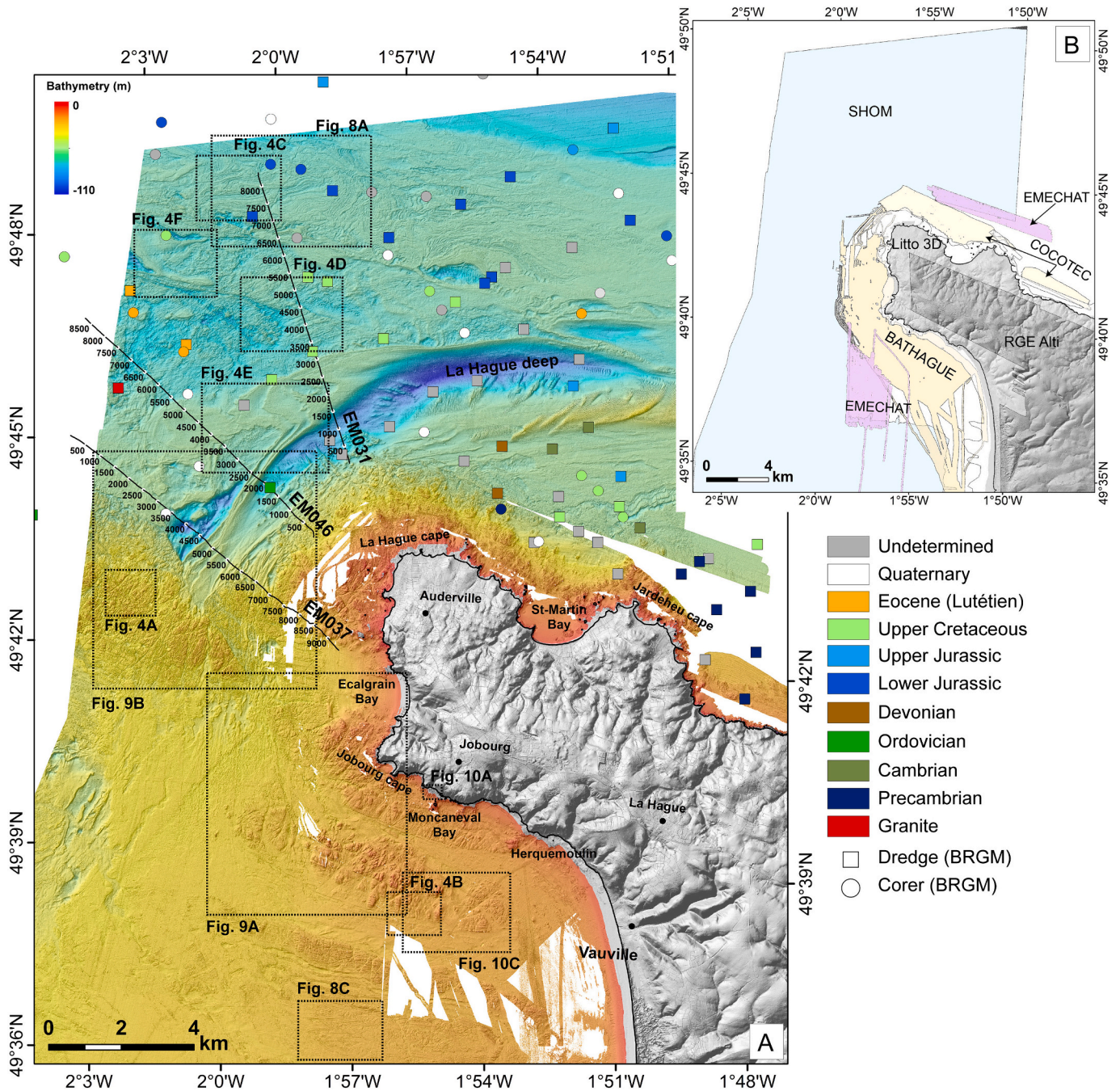


Fig. 3. Onshore/offshore dataset used in this study. (A) Land-Sea Digital Elevation Model of the NW Cotentin area compiling high-resolution bathymetric records. Details are shown on Figs. 4, 8, 9, and 10. The location of the EMECHAT seismic profiles (EM031, EM037, EM046) and BRGM marine sample database (colored rectangles and circles) is shown. (B) Inset showing the location of the onshore and offshore dataset used in this work. See text for details.

central Cotentin area during transgression phases (Klein, 1990; Baize, 1998; Dugué et al., 2009). Later on, the deposition of Plio-Pleistocene sediments in three discrete fault-bounded inland basins (Sainteny-Marchésieux (M), Lessay (Le), Saint Sauveur-le-Vicomte (SV)) and probably in the offshore Ecrehou (Ec) basin (Baize, 1998) was primarily controlled by reactivated N120°E faults, but also N20°E and N70°E faults (Fig. 2a). Conversely, the northern part of the CP area recorded a continuous uplift, estimated at 0.01–0.07 mm/yr from the staircase arrangement of Pleistocene marine terraces (Baize, 1998; Coutard et al., 2006; Padoja et al., 2018) and Neogene raras (Padoja et al., 2018).

3. Methodology

The geomorphological and geological patterns of the offshore CP area were relatively poorly known until the high-resolution bathymetry compilation of Furgerot et al. (2019). Our land-sea structural approach, based on the following data, leads us to improve the knowledge of the polyphased tectonic history recorded by this area since Variscan times.

3.1. Topo-bathymetry data

A continuous land-sea DEM of the CP area has been compiled by merging various available high-resolution topographic and bathymetric data, completed with local high-resolution orthophotos acquired during this work in the shore area (Fig. 3).

Bathymetry data acquired by the SHOM (Service Hydrographique et Océanographique de la Marine) combine single-beam sounder records (resolution lower than 100 m) and multibeam echosounder data collected between 2005 and 2017 (resolution up to 1 m). Additional high-resolution coastal bathymetry acquired by interferometric echosounders onboard the R/V Haliotis (IFREMER) west of La Hague (BATHAGUE cruise, Bailly du Bois, 2010) and north of La Hague (COCOTEC cruise, Duperret, 2019) are also included in the study (Fig. 3). Interferometric data reached a planar resolution of 1 m, after processing based on the GLOBE software (IFREMER). The ca. 2 km-wide coastal fringe is covered by a continuous and high-resolution land-sea altimetry database obtained between 2016 and 2020 during LiDAR (airborne laser) surveys in the framework of the Litto3D project conducted by the SHOM, IGN (Institut National de l'Information Géographique et Forestière) and ROL (Réseau d'Observation du Littoral de Normandie et des Hauts-de-France). LiDAR records have been merged locally with onboard vessel multi-beam echosounder (SMF) along the shoreline to produce a continuous mapping of the coast. Litto3D data combined the shallow-water bathymetry with coastal topographic data with 2 m map resolution and 50 cm elevation resolution.

Onshore and coastal topographic data are extracted from the IGN altimetric database RGE Alti (Référentiel à Grande Echelle) with a planimetric resolution of 1 m. The coastal boundary between land and sea is referred to as a continuous line named TCH (Trait de côte Historique), defined as the maximal high-water level reached during an astronomical spring tide (labelled 120), in normal meteorological conditions. The IGN 69 French altimetric system is used as a base for the common elevation scale in the DEM. The difference between the terrestrial zero (IGN 69) and the local Hydrographic Zero (ZH) is found for the closest referenced SHOM harbour station (Goury) at 4.827 m. All bathymetry data have been corrected with this value using ArcGIS software. Finally, a static -0,3 m correction of bathymetric data is required to compensate for mean sea-level variations associated with the average tidal currents in the Alderney Race (Bailly du Bois et al., 2020). The resulting land-sea DEM of NW Cotentin is referenced in the Lambert-93 projection system associated with the geodetic system RGF 93. The newly-acquired DEM of La Hague Cape, harmonized using the ArcGIS software, covers a 387 km² surface with a mean resolution of 1 to 2 m (Fig. 3). The imagery of the DEM is improved using the hillshade treatment in ArcGIS with illumination sources combining two perpendicular azimuths (45° and 315°) and a constant tilt of 45° (Fig. 3).

3.2. Seismic reflection data

The high-resolution seismic reflection data (HR-sparker) have been acquired during the EMECHAT scientific cruise conducted in June 2022 onboard R/V Côtes de la Manche (IFREMER) (Graindorge, 2022). A total length of 728 km of HR seismic lines has been recorded across the NW Cotentin platform of the English Channel, roughly between Cherbourg and Vauville Bay (Fig. 3), using: (i) a sparker (SIG ©) source with an energy of 250 to 750 J, (ii) the IFREMER 48-channels streamer (GEO Marine Survey Systems©), called THR 150 m, with 24 traces (1 m-spaced) and 24 traces (2 m-spaced) and (iii) the Geo-Suite acquisition © software with a shot interval set at 500 ms, a recording length set at 300 ms and a sample frequency of 10 kHz.

Positioning was obtained using GNSS (Global Navigation Satellite System) with a meter-scale resolution. The seismic data were first processed on board using homemade MATLAB codes and IFREMER SolidQC© software. On board processing includes quality-control operations and basic seismic processing: (i) check integrity of SEG Y data, (ii) single trace edition to check data, (iii) geometry (source, receiver) check, source and streamer drift evaluation, (iv) quality control of signature and noise levels, (v) check and processing of navigation, (vi) computation of sources and receiver positions in a seismic line framework, streamer and source drift correction, (vii) raw SEG Y creation including all shots and channels corrected and positioned in the seismic line reference frame, (viii) binning of seismic data (equivalent to CDP gathering but using real sources and receiver positions), and (ix) stacking of seismic data at constant velocity ~ 1500 m/s in order to obtain the first processed seismic lines. This first processing sequence provides structural images down to ca. -100 m below sea-floor.

The second laboratory sequence includes three main steps: (i) calculation of the semblance every one hundred bins, (ii) two successive velocity analyses in order to determine RMS (Root Mean Square) velocities, and (iii) stacking using pre-determined RMS velocities. This sequence tends to: (i) globally improve the signal/noise ratio, (ii) to enhance the amplitude of reflectors in time depth, and (iii) reduce the amplitude of the multiples taking into account the shallow water context. All the processed lines have then been corrected from the tide effect which is particularly strong in this part of the English Channel. Lastly, seismic lines have been incorporated in the Kingdom (S&P Global) software© for a comprehensive interpretation of seismic units. Three EMECHAT seismic profiles (EM031, EM037, EM046) are selected and shown in this paper for their relevance (Fig. 3a).

3.3. Local orthophotography of the shore platform

Unmanned Aerial Vehicle (UAV) imagery has been acquired at low tide in a specific coastal site, i.e. the Moncaneval bay (Fig. 3a) which shows structural interests during our field works. The UAV (DJI matrice 300 RTK) was equipped with a DJI Zenmuse L1 LiDAR sensor. Post-processing of the image was carried out using Terrasolid UAV software, creating a very high-resolution ortho-mosaic (1 cm in planimetry) imported within ArcGIS 10.8.1 software for detailed interpretation.

3.4. Field structural investigations

Field investigations have been restricted to a few coastal areas which provide accurate geological constraints for a better interpretation of offshore structures identified in the DEM. Important contribution is noticeable for the understanding of the Moncaneval fault zone (Fig. 3a). During this work, striated (polyphased) fault planes have been observed in the Cadomian/Variscan basement material. However, we have decided not to interpret these brittle structures in terms of paleo-stresses because of the long-lasting faulting history experienced by the North Armorican Domain since Late Variscan times up to younger (extensional and/or contractional) events, hence leading in major uncertainties in discriminating each brittle strain episode.

4. Results

Our offshore approach is partly based on the structural analysis of seafloor fabrics identified on high-resolution bathymetric data. The methods used in this work are similar to those previously applied elsewhere in the western part of the Armorican domain, i.e. in the Molène archipelago (Le Gall et al., 2014), in the Morlaix-Tregor area (Le Gall

et al., 2021) and in the South Armorican Domain (Penmarc'h area) (Raimbault et al., 2018).

The morpho-bathymetric map in Fig. 3a reveals the two-fold structural arrangement of the onshore/offshore CP area under study. A southern domain, extending as far north as 49° 45', is strictly composed of pre-Mesozoic basement rocks which form a shallow marine platform with water depths <40 m. To the NW, it is dissected and apparently

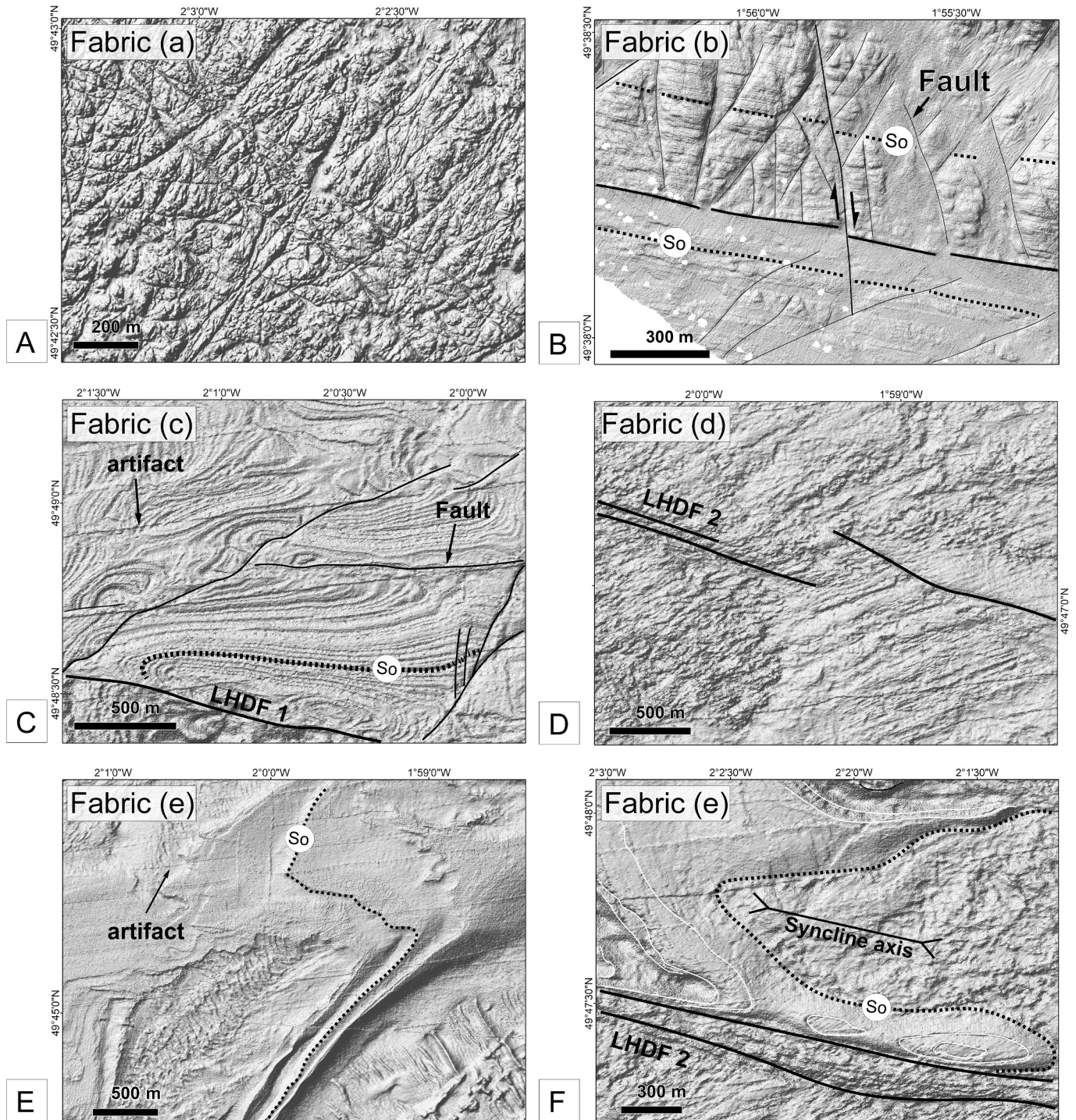


Fig. 4. Shaded relief of the various structural fabrics (a to e) identified from high-resolution bathymetric records on the seafloor west of the Cotentin peninsula. (A) A dense fracture-like network with random orientations, attributed to a granitic bedrock (fabric a); (B) Parallel and closely spaced linear structures interpreted as the trace of bedding (S0) in metasedimentary layered series (fabric b); (C) Regularly-spaced and folded lineations interpreted as deformed sedimentary strata (S0) (fabric c); (D) Scalloped features associated to N70° E-oriented lines, all regarded as inclined sedimentary strata (fabric d); (E and F) Smooth and laterally continuous surfaces corresponding to parallel sedimentary strata (fabric e).

offset by a prominent fault-like structure, oriented at N160°E, the so-called La Hague Offshore Fault (LHOF). In the offshore northern domain, water depths are in the range 50–110 m. There, the morphology of the seafloor is dominated by a prominent arcuate trough-like feature, the so-called La Hague Deep (LHD) that abuts to the west against the LHOF. According to published offshore geological maps (Chantraine et al., 2003), this northern domain coincides with Meso-Cenozoic sedimentary basins. The detailed geological and structural contents of these two contrasting domains are addressed below from a thorough analysis of the seafloor fabrics, then interpreted in terms of lithostratigraphic series. Interpretation is enhanced by cross-analysis of representative seismic profiles and known seabed samples in the area.

4.1. Seafloor fabrics

Texture and coarseness of the seafloor allow to discriminate distinct domains. This approach is chiefly based on: (i) the identification of units and discontinuities expressed by various types of fabrics and later interpreted as geological units and structures; the magmatic or sedimentary natures and tectonic styles of which are defined by correlations with onshore geology, (ii) the age calibration of the inferred series using the marine database (Fig. 3) provided by the French Geological Survey (BRGM, infoterre.brgm.fr), and (iii) cross-correlations with high-resolution seismic data.

4.1.1. Fabric types

Six main types of fabrics (labelled a-f) are recognized from specific structural attributes (Fig. 4) and located on Fig. 3. Whilst the magmatic, metasedimentary or sedimentary nature of the corresponding bedrock is assessed with some confidence, their attribution to specific lithostratigraphic series (and especially about the post-Variscan sedimentary material) is more disputable because of: (i) the modest amount of cored rock samples in the BRGM marine database (Fig. 3a) and (ii) the relatively distant location of onshore exposures which makes difficult any direct lateral correlations. The six types of fabrics are described below from selected demonstrative examples (Fig. 4).

- *Fabric (a)*

The fabric (a) displays a very high ruggedness and is dissected by a dense pattern of fracture-like structures with random orientations (Fig. 4a). By analogy with similar offshore bedrock fabrics previously observed elsewhere in the Armorican marine platform, it is attributed to a magmatic material devoid of any ductile strain.

- *Fabric (b)*

The illustrative example of fabric (b) (Fig. 4b) is located at about 4 km west of Vauville (Fig. 3a). It displays a lower ruggedness and is dominated by a regular and parallel pattern of rather continuous and closely spaced linear structures. This structural arrangement typically evokes a succession of sedimentary (or metasedimentary) strata (S_0) which can be further subdivided into two distinct units as a function of their different bathymetric expression: the northern unit forms a more contrasted relief, composed of a regular pattern of narrow ridges, indicating a mechanically resistant material; the southern unit is more homogeneous and displays a lower and smoother bathymetric expression suggesting a weaker material.

- *Fabric (c)*

The fabric (c) occurs in the northernmost part of the map (Fig. 3a) where it spectacularly expresses by a dense pattern of continuous and regularly spaced lineations, drawing an intricate system of km-scale fold-like structures (Fig. 4c). They are thus confidently interpreted as a thick pile of gently folded sedimentary strata (S_0).

- *Fabric (d)*

The fabrics (d) occur south of the fabric (c) domain in a triangle-shaped area bounded to the west by the LHOF (Fig. 5). They correspond to a dense pattern of scalloped features associated with a system of straight lines globally oriented at N70°E (Fig. 4d). The linearity of these fabrics evokes a succession of sedimentary strata, possibly in an inclined position, the dip direction of which is not firmly established.

- *Fabric (e)*

The fabric (e) corresponds to very smooth and laterally continuous surfaces (Figs. 4e, f) which chiefly occur in two distinct morphostructural contexts (Fig. 3a): (i) to the south in close spatial association with the arcuate LHD feature (Fig. 4e) and (ii) further north, in a narrow fault-bounded syncline oriented at N100°E (Fig. 4f). In the two areas, the terrains corresponding to fabric (e) are locally truncated by erosion, hence revealing their 3D-structure as a succession of parallel strata of sedimentary origin (Figs. 4e, f). However, the contrasting individual strata thickness patterns in the two sedimentary packages (thinner strata in the northern area, Fig. 4f), as well as their mutual structural relationships with surrounding fabrics, lead us to attribute the fabric (e) to two distinct lithostratigraphic units (Figs. 4e, f), in agreement with the age data supplied by the BRGM marine database (following section).

- *Fabric (f)*

All the above mentioned fabric networks are disrupted by linear discontinuities extending with a segmented (or not) trajectory over a wide range of lengths, commonly exceeding a few km's (Fig. 4). These are fault traces which are well expressed when they separate contrasting rocky material. Their direction pattern is dominated by N40°E, N100°E and N160°E subsets. The kinematics and relative chronology of a few of them are discussed below.

4.2. Seismic interpretations and lithostratigraphic attributions

The new offshore geological map of NW Cotentin in Fig. 5 is based on the interpretation of two types of data, i.e. seafloor structural fabrics and seismic reflection profiles. The spatial distribution of the seven seafloor structural fabrics described above leads to elaborate a preliminary map showing juxtaposed domains with specific rocky material. Then, the latter have been interpreted as lithostratigraphic units via various methods. In the southern offshore domain, devoid of Meso-Cenozoic cover, the seafloor fabrics have been directly correlated with the basement series exposed onshore in the CP. In the northern offshore domain, the seafloor fabrics relate to various Meso-Cenozoic deposits which were previously dredged/cored by the BRGM (BRGM marine database, Figs. 3a, 5). Their lithostratigraphic attributions are constrained by a few age data (the reader could refer to <http://geoservices.brgm.fr/geologie> for details), combined to correlations with nearly similar and contemporaneous onshore deposits in Northern France. The accuracy of the inferred ages has been checked by addressing the mutual structural relationships of the dated series on three selected EMECHAT seismic lines (Fig. 7). Special attention has been paid on the specific seismic character of each sedimentary unit (Fig. 6), as well as on the conformable vs unconformable nature of their mutual contacts. Fruitful informations are also obtained about the deep geometry and (inferred) nature of the fault network identified on the seafloor (fabric f, Fig. 4). These cross-lines, nearly orthogonal to the arcuate regional structures, penetrate as deep as 100 ms below sea-floor on the Two-Way travel Time (TWT) seismic sections, i.e. approximately one hundred meters below sea-floor using a 2000 m/s Vp.

The new geological map of the NW offshore CP area (Fig. 5) greatly differs from previously published maps (Chantraine et al., 2003 and references therein; Furgerot et al., 2019) as it provides an improved

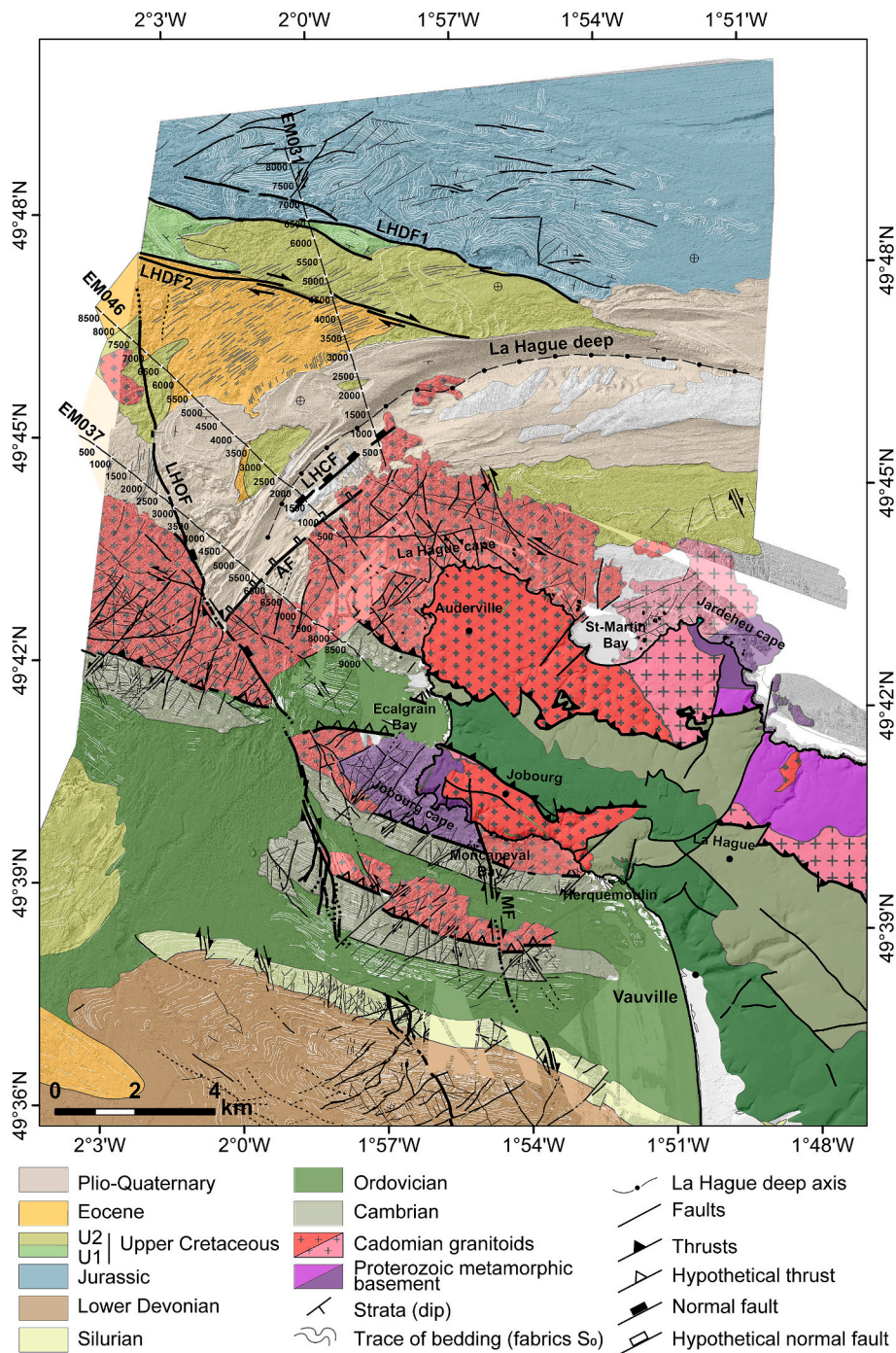


Fig. 5. Onshore/offshore geological map of the NW Cotentin peninsula. The onshore map is simplified from published 1: 50000 geological maps. The offshore map (this work) is obtained from compiled and newly-acquired high-resolution data. The trace of the three EMECHAT seismic lines in Fig. 7 is shown. LHDF: La Hague Deep fault; LHOF: La Hague Offshore fault; LHCF: La Hague cape fault; AF: Auderville fault; MF: Moncaneval fault.

picture of both the Cadomian/Paleozoic and Meso-Cenozoic structural patterns and also reveals first-order tectonic structures unknown before (see Section 4.3).

4.2.1. The pre-Mesozoic basement series

The fabric (a) has been attributed to magmatic material. Therefore, the only potential candidates exposed onshore are the Auderville, Thiebot and Greville Cadomian granites which similarly show a rough morphology and are further cut by a dense fracture network (Figs. 3a, 4a). The interpretation of fabrics (a) as Icartian migmatites is not favored because there is no offshore evidence of any regular and planar

structures commonly displayed by these rocks.

The two sub-facies discriminated above in the fabric (b) pattern pass laterally eastwards into onshore Paleozoic meta-sedimentary rocks exposed in the Ecalgrain bay (Figs. 3a, 5). The more resistant material forming the northern offshore substratum fits the Cambrian sandstones involved in Variscan southerly-verging fold-thrust structures (Fig. 5). The weaker offshore material to the south correlates with the overlying Ordovician (and eventually Silurian) schist/sandstone alternations, known to be more sensitive to erosional processes (Fig. 5). Whatever its position on the EMECHAT seismic lines, as being either exposed on the seafloor or overlain by Meso-Cenozoic deposits, the basement is imaged

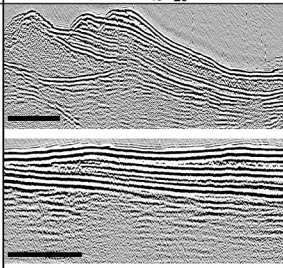
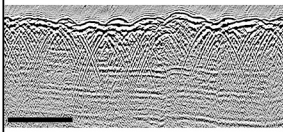
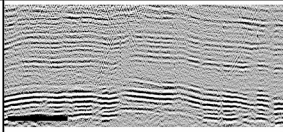
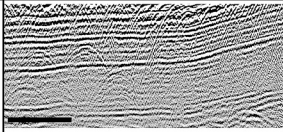
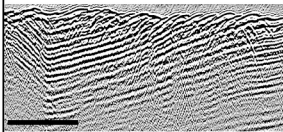
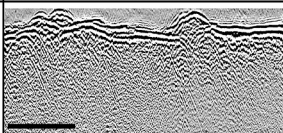
Facies	Example Vertical exaggeration x 5 1° 5° 10° 45° 20° 100m	seismic attributes		Internal structure
		Amplitude	Continuity	
Plio-Quaternary		L / H	L / H	Oblique subparallel or sigmoidal prograding (Onlap & dowlap limits)
		H	H	Parallel aggrading (Toplap)
Eocene		L / M	M	Subparallel or chaotic
Upper Cretaceous (U2)		M / H	M / H	Parallel aggrading concave / convex-up
Upper Cretaceous (U1)		L / H	L / H	Parallel divergent associated with chaotic facies
Jurassic		H	H	Oblique and parallel to steeply divergent reflections
Crystalline basement		L	L	Chaotic

Fig. 6. Geological units identified on EMECHAT seismic profiles from their seismic characteristics. The amplitude and continuity of the reflectors are qualitative attributes, assessed with three confidence levels: high (H), medium (M), low (L).

as a chaotic facies with a relatively low amplitude, confidently attributed to the crystalline rocks (possibly Cadomian granitoids in Figs. 6, 7).

4.2.2. The post-Variscan sedimentary series

According to the BRGM marine database (Fig. 3a), the folded sedimentary series expressed by the fabric (c) (Fig. 4c) north of LHDF1 correspond to limestones and marls which yielded Lower Jurassic (Toarcian) ages. They likely correlate with slightly younger Jurassic sequences exposed on the foreshore of the Cape Gris-Nez, eastern Channel (Fig. 8b) and similarly involved in large wavelength synclines-anticlines (Lamarche et al., 1998; Deconinck and Baudin, 2008). On the seismic line EM031 (Fig. 7a), these series are imaged as a relatively homogeneous package, > 75 ms-thick (75 m using a 2000 m/s Vp), of parallel and regularly spaced reflectors, showing a high amplitude and high continuity (Fig. 6), and involved to the north in a southerly-facing monocline. Along the southern limb of the structure, the strata pattern is involved in a dense network of ~200 m-scale upright synclines/anticlines, as far south as a blind seismic zone, about ~300 m-wide, attributed to the steeply dipping LHDF1. The Jurassic series are suspected to lie at depth on the two others seismic lines EM037 and EM046. Since their basal contact with the basement is not observed, their total thickness remains unknown.

Immediately south, the 2 km-wide LHDF1/LHDF2 faulted corridor (Fig. 5) is mostly occupied by the scalloped fabric (d) (Fig. 4d). At the

western extremity of the corridor, this material occurs in the core of a N100°E-oriented syncline, on top of a smooth and well-stratified material (fabric (e), Fig. 4f). Rock samples cored by the BRGM (Fig. 3a) in the two contrasting material both yielded Upper Cretaceous ages (BRGM database), while the scalloped material (fabric d) was identified as chalk. On the seismic line EM031 (Fig. 5), the two Upper Cretaceous sub-units, named here U1 and U2, form a > 100 ms TWT assemblage of alternating low, medium to high parallel reflectors (See Fig. 6 for details), in a flat-lying position (Fig. 7a). The two sub-units are separated by high amplitude reflectors at the base of U2, whereas U2 contains stronger amplitude reflectors (Figs. 6 and 7a, b). The Upper Cretaceous strata are slightly down-flexed and up-flexed as approaching the LHDF2 and LHDF1 structures, respectively (Fig. 7a). On EMECHAT seismic line EM031 (Fig. 7a), the Cretaceous series are supposedly covering unconformably the Jurassic sequences. At the southern end of the EM046 line, they directly overlie the granitoid basement (Fig. 7b).

In the broad sedimentary domain extending south of the LHDF2 (Fig. 5), cored rock samples from the extensive domain with the fabric (d) correspond to shallow-water bioclastic carbonates of Eocene ages (BRGM database, Fig. 3a). These lithostratigraphic attributions are confirmed on the seismic lines EM031 and EM046 (Fig. 6a, b) where these layers overlie conformably the topmost Upper Cretaceous reflective sequences (see above). On these lines, Eocene formations correspond to weakly stratified (locally moderately chaotic) package of

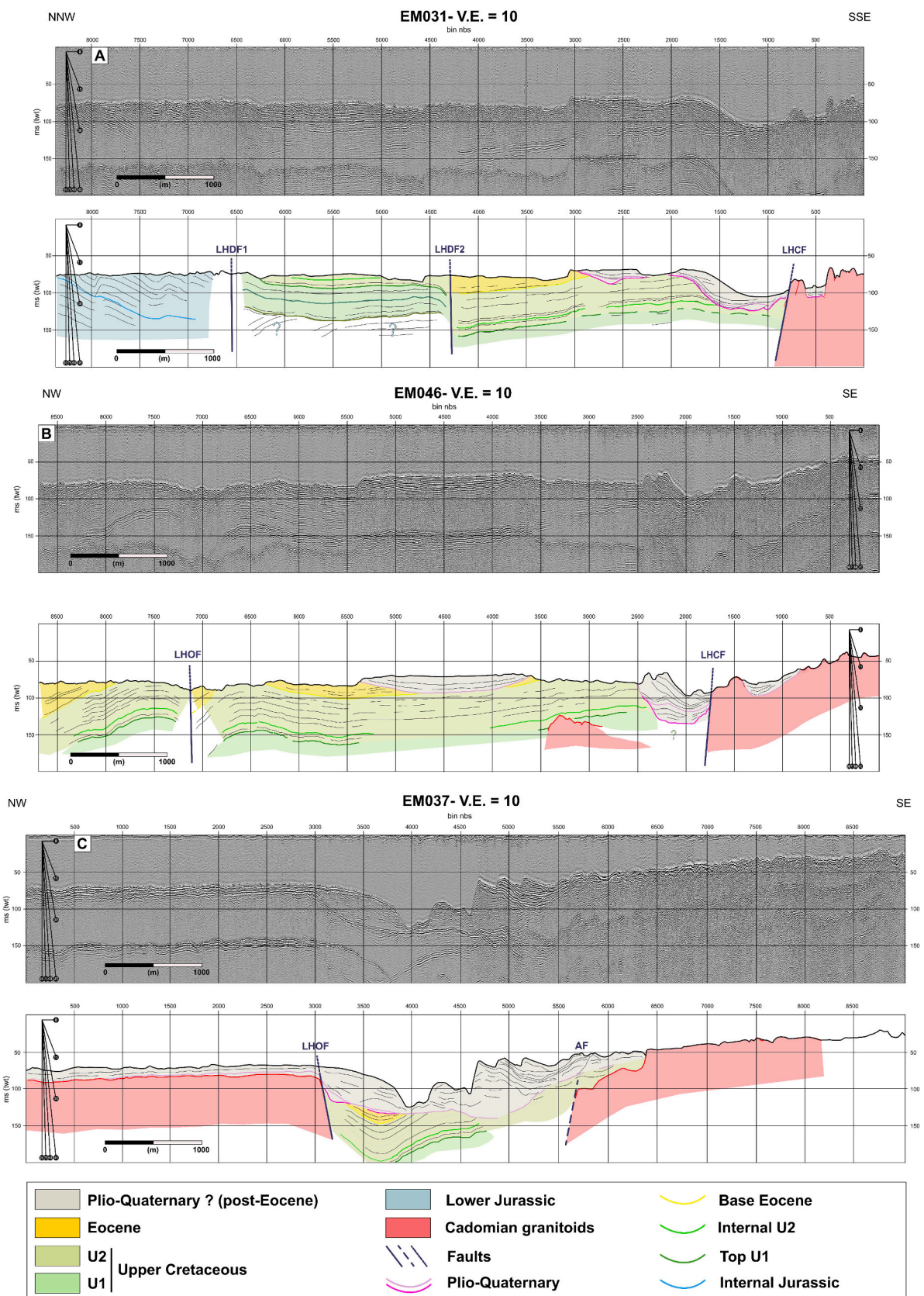


Fig. 7. EMECHAT cruise seismic profiles. Uninterpreted and line drawings of EM 031, EM 046 and EM 037 sections, with an indicative scale of the true dips as a function of the chosen vertical exaggeration (10). Vertical scale is in two-way-travel time (twt) in ms. Horizontal scale is the number of bins. Location on Figs. 3, 5.

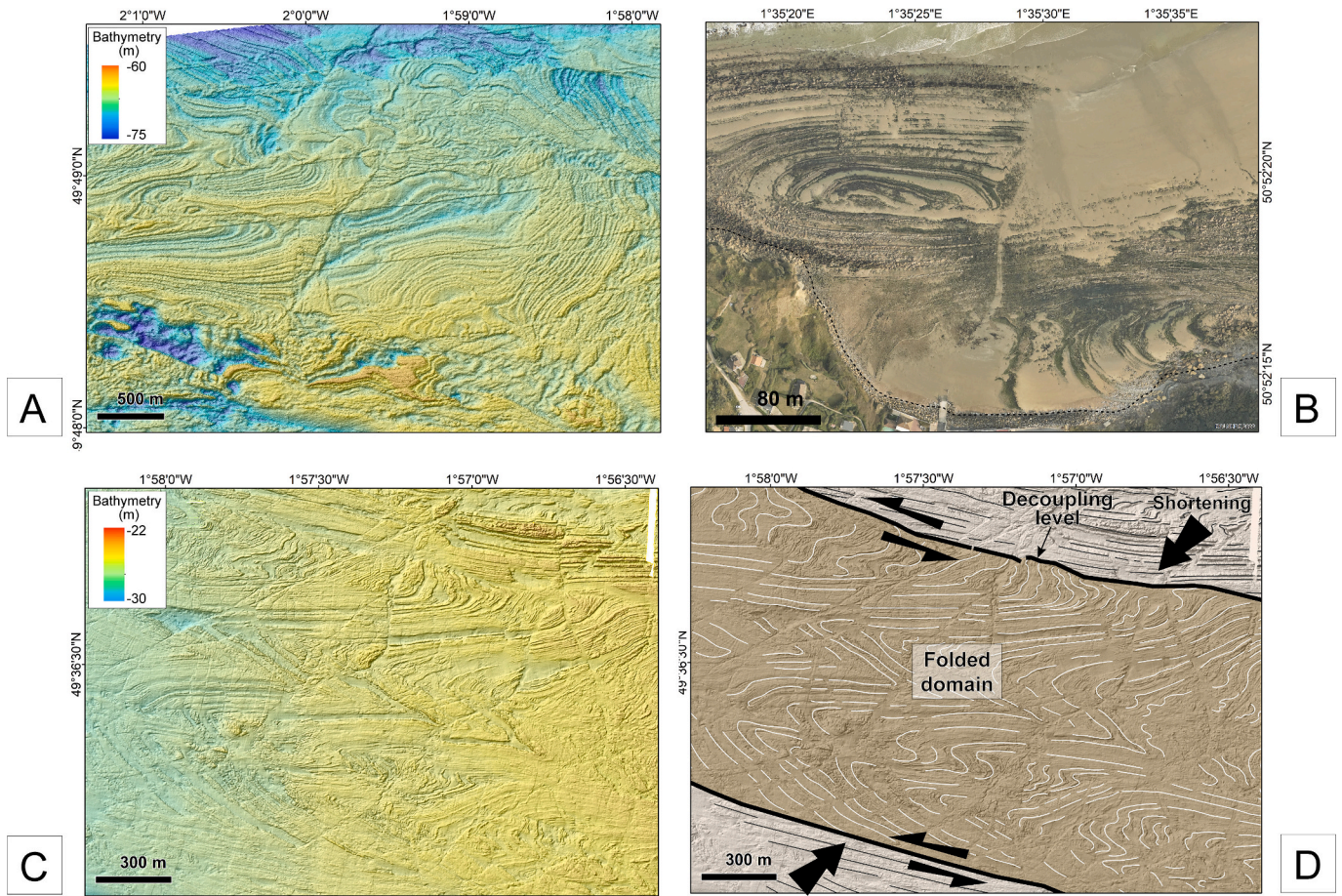


Fig. 8. Tectonic style of ductile deformations identified in offshore series from high-resolution bathymetric data, west of the Cotentin peninsula. (A) A dense pattern of fold-like structures in Jurassic sedimentary series in the northernmost part of the study area. (B) Nearly similarly folded Jurassic strata in the foreshore of Cape Gris-Nez, Boulogne-sur-Mer, Hauts-de-France region, northern English Channel (aerial orthophotography, IGN). (C) Intensely folded Devonian strata in a spatially-restricted faulted corridor, south of the study area. (D) Interpreted model of Fig. 8c showing two decoupling sinistral shear zones in a transpressional framework. Location on Fig. 3.

parallel reflectors (low amplitude) with an apparent gently northerly-dipping attitude (Figs. 6 and 7a, b).

In the vicinity of the LHD arcuate structure, a regularly-organized succession of strata, i.e. the seafloor fabric (e) in Fig. 4e, overlap the N70°E structural grain in both the Cretaceous and Eocene series (Fig. 5). On the seismic lines EM031 and 46, these post-Eocene series occur as a lens-shaped body of high amplitude reflectors (Figs. 6 and 7a, b) arranged in various ways as forming either parallel aggrading reflectors or imbricated oblique, sub-parallel to sigmoidal reflectors with numerous internal onlap and downlap terminations (Figs. 6, 7). At depth, this unit is bounded by a basal erosive surface truncating as deep as the Upper Cretaceous deposits so that the latter are currently exposed on the seafloor via erosive windows (Figs. 5, 7a). The interpretation of these post-Eocene deposits as Plio-Quaternary fluvio-glacial sequences (Fig. 3, BRGM marine database) is supported by correlations with similar seismic/stratigraphic patterns in English Channel deeps (Lericola et al., 2003). In addition, Oligocene and Miocene bioclastic deposits are restricted to narrow depressions in the Sainteny-Marchésieu basin (SM, Fig. 2a) inland: there, widely preserved sedimentary sequences have been dated between Pliocene and Quaternary (Dugué et al., 2009).

4.3. Structural analysis

Merging vertical (seismic) (Fig. 7) and map data (Figs. 3a, 5) helps us to perform a thorough and multi-scale structural analysis of the onshore-offshore studied area, as focusing on the regional structural pattern and

a number of specific structures and then as proposing a temporal framework of deformation.

4.3.1. The regional structural pattern

To the south, the structural arrangement of the Paleozoic/Cadomian substratum is dominated by km-wide alternating bands of Cambro-Silurian series and granite/migmatite rocks (Figs. 2b, 5). These series are involved onshore in a N100°E-trending syncline (Jobourg-Siouville) and thrust pattern (Dissler and Gresselin, 1988; Graindor, 1998). This fold/thrust system likely extends westwards offshore with a consistent spacing and orientation pattern, before abutting against, or being dextrally offset by the N160°E LHOF structure. The offshore extent of the thrust network is only hypothesized because of the lack of supporting evidence on the bathymetric data. The northernmost granite belt (Auderville) displays a more intricate map-scale pattern. Its structure is composed of two parallel (N100°E) bodies further connected via a short and narrow N40°E segment and cut by the LHOF. West of the LHOF and south of the granitic body, the offshore compartment is principally occupied by Cambro-Ordovician series. The thrust contact between the two units is hypothesized.

To the north, the lithostratigraphic/structural organisation of the post-Variscan offshore basinal area shows three distinct domains (Fig. 5). (i) To the north, the Jurassic series correspond to a well-stratified limestone/marl package involved in a few 100 m's-scale fold system (see below). They are tectonically juxtaposed to the south to (ii) a 2 km-wide fault-bounded block, limited by the N100°E-oriented LHDF1

and LHDF2 structures and composed of Upper Cretaceous chalk series, further involved to the west in a gentle fold syncline (see below). (iii) South of the LHDF2, extensive Eocene bioclastic carbonate series, underlain by Upper Cretaceous deposits, display an arcuate structural grain which swings from N40°E to N70°E eastwards. These series are locally deeply incised and unconformably overlain by post-Eocene sedimentary series (Fig. 7) which abut on the LHOF. These series, possibly Plio-Quaternary in age, are intensely eroded, especially along the arcuate LHD feature. These recent sedimentary and morphological features are

limited to the SW by two nearly orthogonal basement (granitic) fault blocks along the LHOF (N160°E) and the inferred N40°E AF (EM037, Fig. 7c).

4.3.2. Specific structures

- Fold structures

Three distinct types of fold patterns are distinguished from their

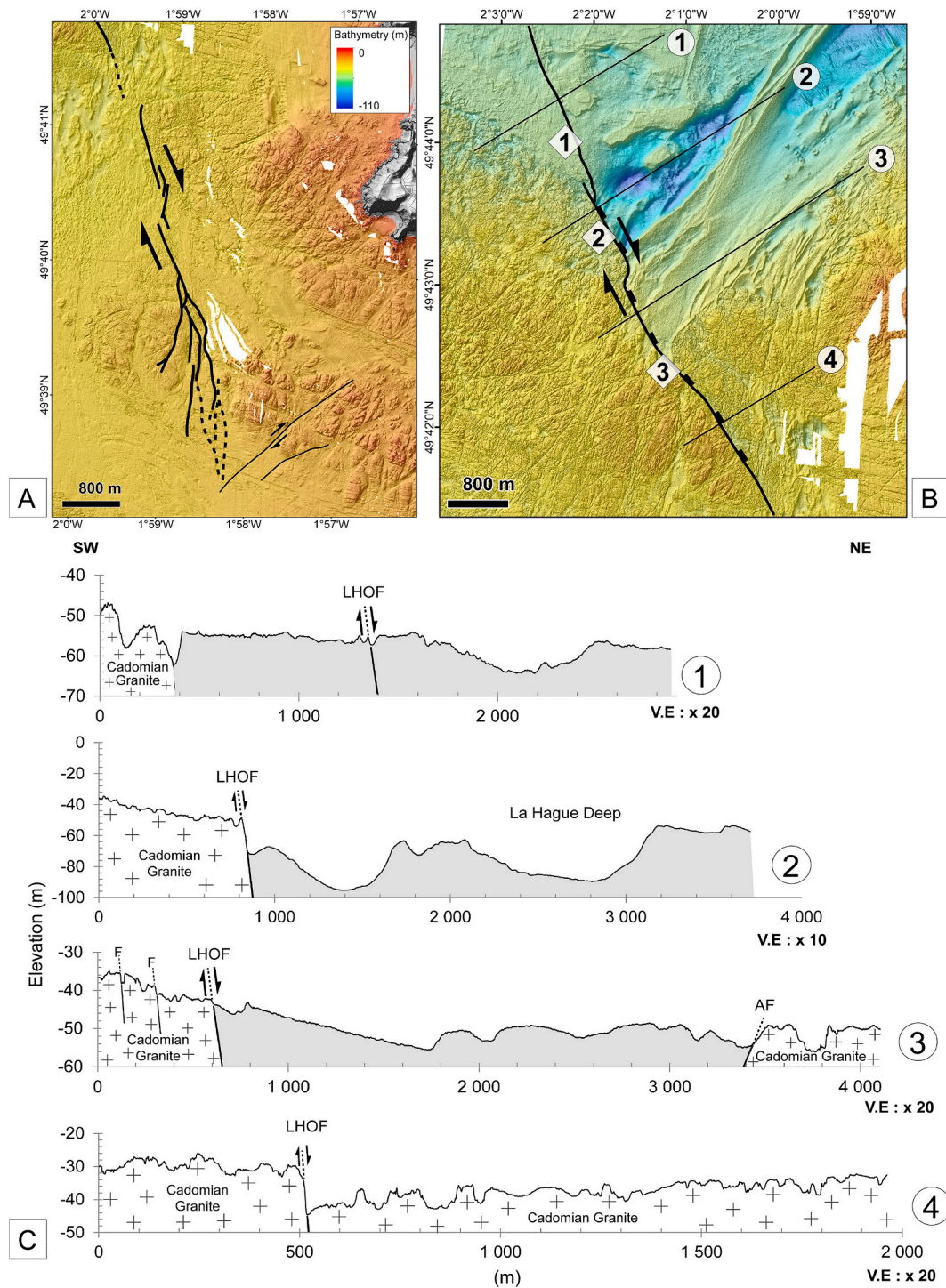


Fig. 9. The La Hague Offshore fault (LHOF). (A) The anastomosed structure of the southern trace of the fault on the high-resolution DEM. (B) The segmented structure of the LHOF to the north, with three hard-linked dextral segments. (C) The topographic profile of the LHOF on four seriated bathymetric cross-sections. Location on Fig. 3.

contrasting map geometry and spatial distribution. The two first patterns are confidently related to post-Eocene deformations whereas the third one is obviously Variscan in age because of the ductile type of the corresponding deformation.

(i) One of the most impressive structural features on the North Contentin bathymetric map in Figs. 3a, 4c, 8a is the trace of a fold network expressed in the Jurassic sedimentary series to the north; these folds are dissected by discrete N50–70°E faults (Fig. 8a). These km-scale fold structures display various map geometries, ranging from tight to open folds, and with axial directions swinging between N-S and N100°E (dominant) (Figs. 4c, 8a). Where partly eroded, their hinge zones show fold axes plunging shallowly to the WNW or to the ESE. The asymmetry expressed by short vs long fold limbs does not provide firm evidence about senses of associated lateral shearing. On one other hand, the arcuate map trace of a few fold hinge zones is kinematically compatible with a component of dextral shearing during folding. Dextral kinematics also expresses by a network of later (post-folding) subsidiary faults, parallel to the LHDF1/LHDF2 bounding structures. The map fold pattern suggests a relatively high intensity of strain, in contradiction with its seismic image which conversely shows large wavelength and gently dipping syncline/anticline folds (EM031, bins 6500–8500, Fig. 7a).

(ii) The Cretaceous chalk series (U1/U2) occurring in the 2 km-wide faulted corridor (LHDF1 and LHDF2) further south are involved in a large-scale syncline, oriented at N100°E, with gently dipping flanks (a few degrees) (Figs. 4f, 5, 7a). Its shallowly plunging axis (to the ESE) is clearly expressed to the west in its partly eroded hinge zone (Fig. 4f). In this corridor, Cretaceous sequences (U1) are locally affected to the west, along parts of the two bounding faults (Fig. 7a), by much tighter anticline fold structures displaying shallowly-plunging curved axes (Figs. 4f, 5, 7a).

(iii) The southernmost part of the offshore studied area shows intensely folded Devonian strata, spatially confined within a ca. 4 km-wide zone parallel to the N100°E regional structural grain (Fig. 8c). The consistent asymmetry of the Z-type fold traces (drawn by long vs short limbs) indicates a component of sinistral ductile shearing during folding. The restricted spatial distribution of folding necessarily implies two decoupling levels acting as sinistral shear zones on both sides of the folded zone (Fig. 8d). Both folding and shearing likely operated in a Variscan transpressional setting, in response to a NE-SW-directed regional shortening (Fig. 8d).

- *The La Hague offshore fault (LHOF)*

The LHOF is a ca. 15 km-long discontinuity which extends at N160°E, a few km off the coast, through both Meso-Cenozoic and substratum terrains (Figs. 3a, 5, 7b, c, 9). It is a composite structure, comprising a series of segments, which displays an increasing complexity towards its southern tip in stratified Paleozoic series. Southwards, the linear trace of the LHOF splits into splaying and anastomosed faults forming a submeridian and < 1 km-wide fault zone cutting through Cambro-Ordovician strata as far south as a tip located approximately at N49°38' (Fig. 9a). The drag-fold structures present along parts of these subsidiary faults indicate a component of dextral displacement, not estimated because of missing stratigraphic markers (Fig. 9b).

Its northern map-trace includes three colinear segments, ca. 4 km-long each, arranged in a right-stepping pattern. These segments connect via either an overlapping zone (segments 1 and 2) or a bend (segments 2 and 3) (Fig. 9b). The bathymetric signature of the LHOF dies out northwards beneath the Eocene cover so that its relationships with the LHDF2 remain unknown (Fig. 5). Close to its inferred northern tip point, the LHOF behaves as an oblique fault with a vertical component imaged on the seismic profile EM046 (Fig. 7b), combined to a dextral component evidenced in map-view by the offset of the Eocene-Cretaceous boundary.

On seriated bathymetric profiles crossing the western boundary of

the LHD, the LHOF expresses by a < 20 m-high morphological scarp facing eastwards (Fig. 9c). Maximum height values are observed along the segments 2 (in the LHD) and 3 (intra-basement). On the seismic reflection profile EM037, the easterly-dipping LHOF separates two contrasting structural blocks (Fig. 7c). The western block is chiefly composed of the offshore Auderville granite and a thin (a few meters) cover of Plio-Quaternary sediments. The latter thicken dramatically (~20 m-thick) eastwards in the LHD downthrown block where they unconformably overlie gently folded Eocene and Upper Cretaceous series. These hangingwall series are involved in a large-scale drag fold-like structure possibly resulting from the downthrow of the LHD block along the fault. The constant thicknesses (time-sections) of Eocene and Upper Cretaceous series in the immediate hangingwall of the fault are not compatible with its activity during the deposition, but rather suggest its post-Eocene reactivation with an apparent normal movement (Fig. 7c).

- *The Moncaneval fault*

South-East of the Jobourg cape onshore (Figs. 3a and 5), Icartian migmatites are tectonically juxtaposed to the east to a foliated Cadomian granodiorite (Thiebot) along the so-called Moncaneval fault zone (MFZ) oriented at N160°E (Figs. 10a, b). The contact is a steeply-dipping fault zone, ca. 10 m-wide, which cuts through unstrained submeridian doleritic dykes, dated at 380 to–350 Ma (K/Ar, Leutwein et al., 1972), and hosted by the granodiorite (Figs. 10a, b). The sigmoid tectonic fabrics present within the fault zone indicate dextral ductile shearing that we relate to a Variscan event (Figs. 10a'). The MFZ continues southwards offshore as an apparent brittle fault, referred here to as the Moncaneval strike-slip fault (MF), which causes the dextral offset (~100 m) of the Cambro-Ordovician/granite thrust pattern (Figs. 5, 10c, d). The MF structure is spatially associated with a (conjugate) pattern of N60°E-oriented faults showing sinistral offsets <100 m (Figs. 10c, d). At a wider scale, the MF and LHOF structures extend as two parallel *en echelon* faults separated by a 4 × 3 km overlapping zone (Fig. 5).

- *The N100°E transverse fault network*

The Meso-Cenozoic series to the north are disrupted by two segmented faults, > 10 km-long each and oriented at N100°E, i.e. the LHDF1 and LHDF2 structures (Figs. 4c, d, f, 5, 7). The LHDF1 is composed of three sinuous overlapping segments. The 0.5 × 2 km overlapping zone connecting the two western segments limit a strip of Cretaceous series (U1 in Fig. 7) involved in a tight anticline fold (see above). Evidence for a component of dextral movement along the LHDF1 is locally argued by drag-fold structures developed in adjoining Upper Cretaceous strata (Fig. 4c). The LHDF1 is sealed to the east by post-Eocene sequences filling up the LHD (Fig. 5).

The southern fault LHDF2 shows structural similarities with its northern counterpart as: (i) being composed of three overlapping segments, (ii) displaying dextral displacements deduced from local drag-fold pattern in the fabric (d) to the south, (iii) being associated with a tight shear-related anticline structure and (iv) being sealed and post-dated to the east by post-Eocene sequences. On the seismic cross-profile EM031 (Fig. 7a), the two faults are imaged as ~200–300 m wide 'blind' zones which typically evoke damage fault zones. Their vertical attitude is consistent with their strike-slip nature inferred above from map-scale evidence. However, the existence of additional vertical offset is argued by the up- and down-flexed geometry of the Cretaceous and Eocene strata along the faults. An apparent vertical offset of 50 ms is recorded by the downthrown block south of LHDF2 whilst an anomalous contact is observed between Lower Jurassic and Upper Cretaceous series along LHDF1 (Fig. 7a).

- *The La Hague Deep (LHD)*

The prominent morphobathymetric expression of the LHD, north of

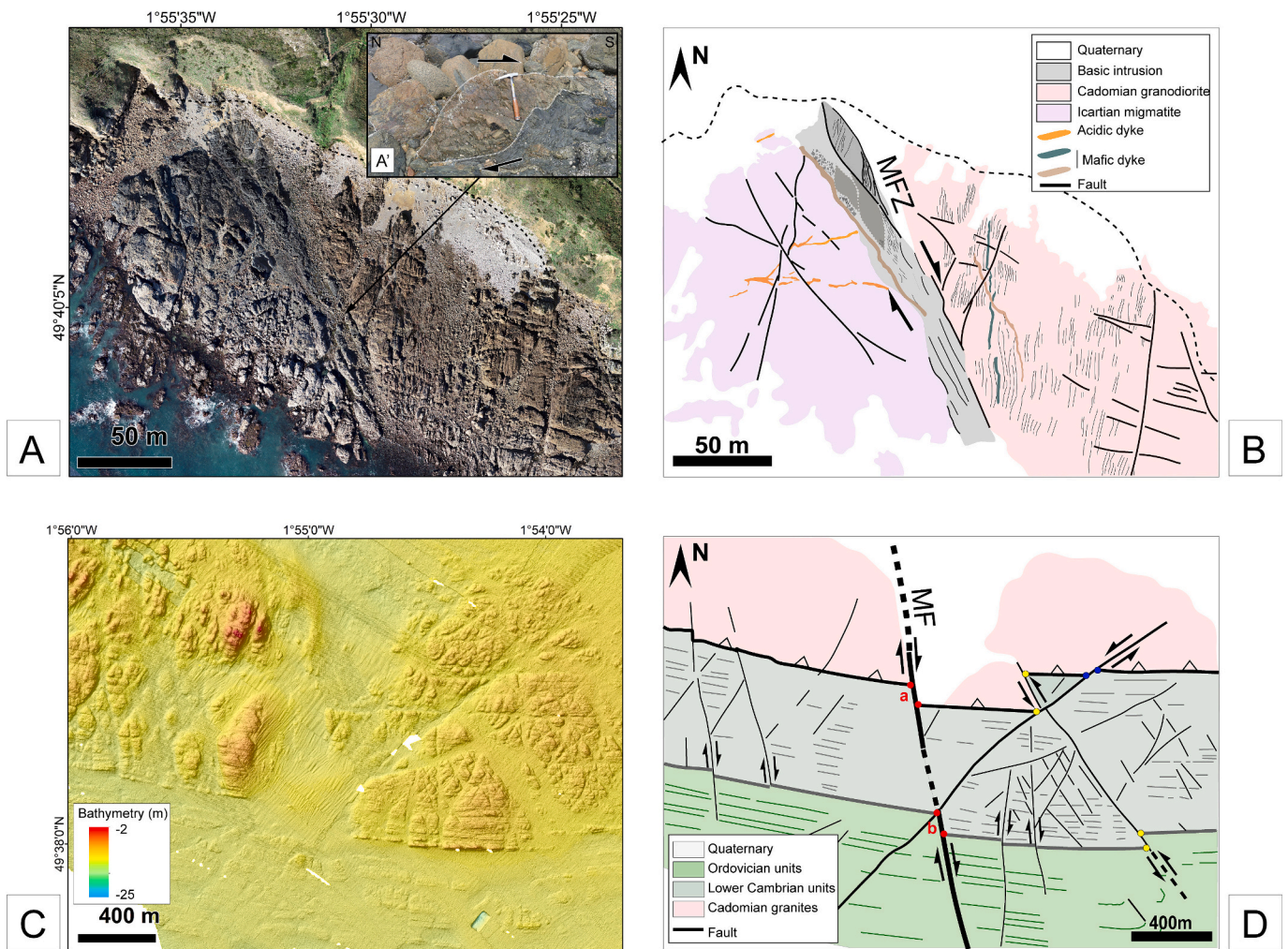


Fig. 10. The onshore-offshore extent of the Moncaneval fault (MF). (A) Very high-resolution (1 cm) Uninhabited Aerial Vehicle (UAV) imagery showing the map trace and structure of the Moncaneval fault zone in the Moncaneval Bay. (B) Structural interpretation of the Moncaneval fault zone as a dextral ductile shear zone. (C) Evidence of a conjugate strike-slip fault network in Cadomian/Paleozoic offshore series, south of the Moncaneval Bay. One of the N160°E dextral fault (MF) extends in the southern prolongation of the Moncaneval fault zone, with lateral displacement <100 m. Location on Fig. 3.

the La Hague cape (Figs. 3, 5), suggests at first approximation that it originates from first-order depositional and erosional processes, further partially guided by the basement structural pattern. When addressing its 3D-morphology, and more especially its vertical dimension (Fig. 7), it is suggested that (i) the LHD probably developed in Plio-Quaternary times as a U-shaped incision displaying a vertical amplitude of 50 m below seafloor and (ii) its infilling sequences were in turn deeply incised by more recent hydrodynamic processes (Fig. 7c). The initial incision followed the N40°E faulted margin of the Auderville granite to the SE and abuts westwards against the N160° LHOE transverse structure (Figs. 7b, c). To the east, the morphological axis of the LHD no longer follows the northern edge of the granite but swings clockwise to parallel the regional N100°E structures.

4.3.3. Chronology of deformation

The orogenic evolution of the Proterozoic/Paleozoic substratum exposed onshore in the CP area has been extensively investigated by previous authors (see references above). The main new insights acquired during this work chiefly concern the structural events (basin and inversion processes) which have affected the W/NW offshore extent of the CP in Meso-Cenozoic times. Due to the poorly-constrained stratigraphic attributions of the offshore sequences, the proposed temporal pattern is approximate, but allows to establish correlations with the adjacent Meso-Cenozoic basins in the English Channel. The proposed

post-Variscan structural events are presented below in an ascending chronological order (Fig. 11).

The oldest tectonic event post-dating the Variscan ductile strain stage corresponds to a strike-slip fault pattern cutting preferentially through Cambro-Ordovician strained (meta)sedimentary series in the southern part of the studied area (Fig. 11a). It comprises two sets of faults, oriented at N40°E and N160°E, and displaying sinistral and dextral displacements, respectively. These brittle structures likely represent a Late Variscan conjugate fault pattern initiated in response to the counterclockwise rotation of the regional shortening from NE-SW (Variscan ductile transpressional stage, folded Devonian strata in Figs. 8c, d) to N-S. During this brittle stage, strain may have focused along preferential structures, such as the N160°E-oriented MF and proto-LHOE dextral structures (Figs. 9, 10). This Late Variscan fault network (commonly labelled Kerforne-type in the Armorican massif) has affected the entire Variscan belt in Armorica as early as Late Carboniferous (Bois et al., 1991; Rolet et al., 1994; Bessin et al., 2017).

The second structural event relates to the deposition of Jurassic sediments to the north (Figs. 5, 11a, b). These dominantly carbonate series are thought to have been deposited in a main depocenter controlled to the south by a N100°E-trending extensional fault, facing to the north (proto-LHDF1). This interpretation is supported by the restricted spatial distribution of the Jurassic sequences which are absent further south as approaching the granitic basement, directly overlain by

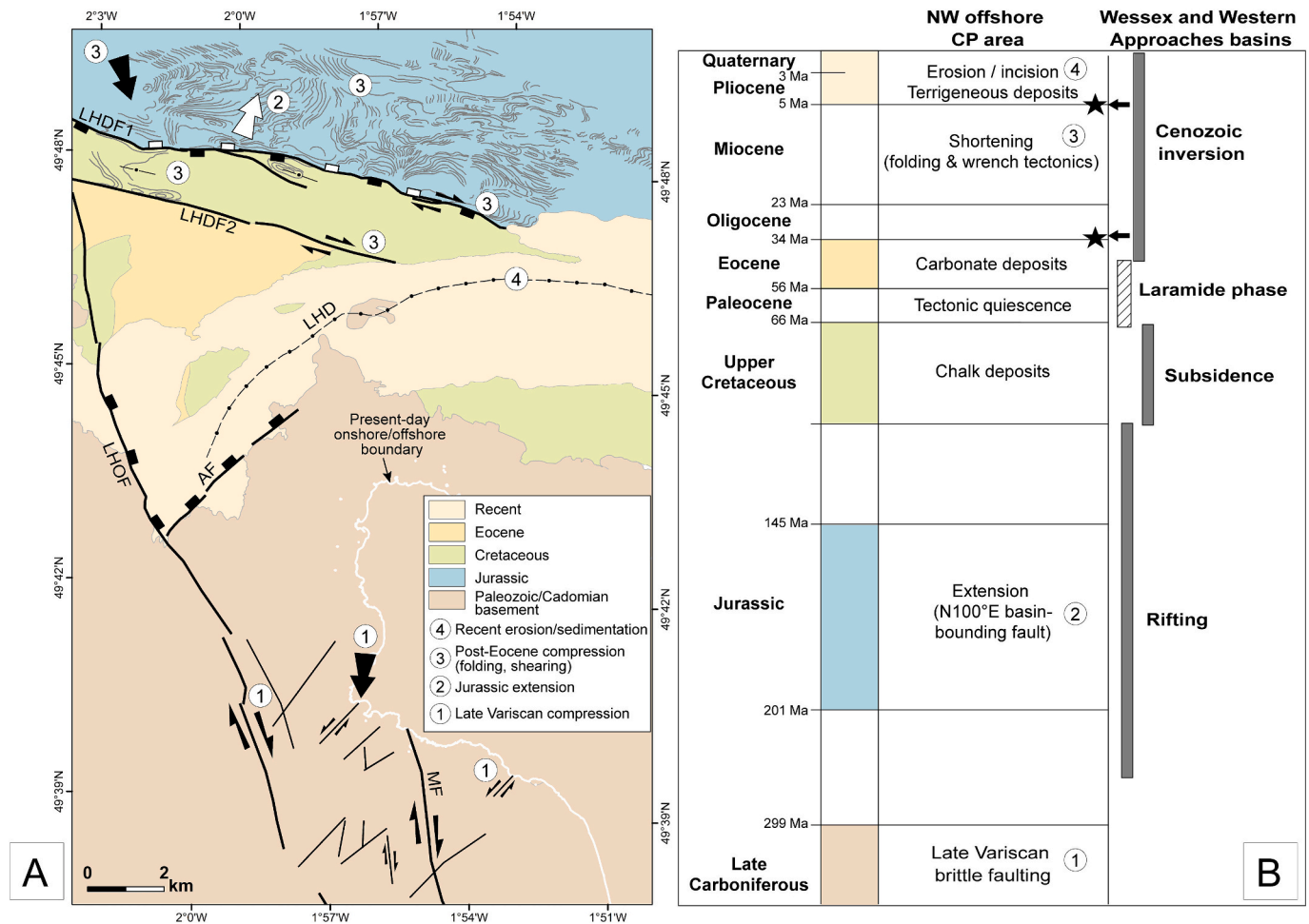


Fig. 11. Tectonic events (in the time-range Upper Paleozoic-Recent) in the NW offshore Cotentin area and correlations to nearby areas in the English Channel. (A) Spatial distribution of both extensional and compressional deformations in the NW offshore extent of the Cotentin peninsula (this work). Same abbreviations as in Fig. 5. (B) Structural events (shown in a simplified stratigraphic column) in the NW offshore extent of the CP area (this work) and in the Channel Basin (modified from Lake and Karner, 1987; Vandycke and Bergerat, 2001; Vandycke, 2002). Numbers refer to events in Fig. 11a.

Cretaceous deposits (Figs. 7b, c).

The following event corresponds to the deposition of Cretaceous (chalk)-Eocene (carbonate) sediments, currently preserved further south within (i) the LHDF1/LHDF2-bounding corridor (Cretaceous) and (ii) a V-shaped faulted block (Eocene) dissecting the Auderville granitic basement (Fig. 11a). This structural pattern leads to question the relative timing of the onset of faulting. The apparent constant thickness of deposits in the immediate hangingwall of the N160°E LHO (see above) suggests the post-Eocene age of the latter (Fig. 7). A similar origin is hypothesized about the AF and LHDF1/LHDF2 structures.

The long-lasting (Jurassic-Eocene) depositional history is followed by a major contractional event, preferentially expressed in the Jurassic and Cretaceous terrains to the north (Figs. 5, 7). Folding and coeval dextral shearing along the LHDF1/LHDF2 bounding fault system are kinematically compatible with a transpressional context recording a NW-SE shortening (Fig. 11). The lack of angular unconformity between Upper Cretaceous and Eocene units on the seismic lines (Fig. 7) suggests that the regional transpression occurred in post-Eocene times, but prior to the deposition of unconformable series, probably Plio-Quaternary in age, sealing the strike-slip faults to the east in the LHD (Figs. 5, 7). The map-scale curvature of the Upper Cretaceous/Eocene series further south is attributed to the indenter effect of the Auderville basement edge during regional shortening.

The youngest structural event experienced by the CP marine platform corresponds to the relatively deep incision of the seafloor during

undetermined low sea-level stages in Plio-Quaternary times (Fig. 11). That resulted in initial excavation of the proto-LHD, then partly filled with fluvio-glacial deposits (Figs. 5, 7). The present-day incised morphology of the latter is confidently attributed to high-energy hydrodynamic processes along the proto-LHD network.

In addition, the seismic sections suggest that the oldest part of the possibly Plio-Quaternary pack could be affected by the LHO. This would be consistent with the preservation of the morphological expression of the LHO.

5. Discussion

The local vs regional significance of the structures identified in the NW Cotentin onshore/offshore area is discussed below in the enlarged framework of the Southern/Central English Channel Meso-Cenozoic basins (Fig. 1). Correlations between these two basinal templates show striking similarities, but also marked differences in terms of types and chronology of deformations. With respect to most previous works devoted to the English Channel offshore basins, one major contribution of our onshore/offshore study is to provide robust data that help discussing the importance of structural inheritance in a typically polyphase tectonic setting involving both basement and younger basin structures.

The onshore structural arrangement in the North Cotentin peninsula is dominated by a Variscan southerly-directed thin-skinned fold/thrust belt with structural trends rotating clockwise from N70°E to N110°E

westwards in the offshore domain (Fig. 2a). These structures likely nucleated along deeply-rooted Archean/Cadomian thrusts to the north (Dissler and Gresselin, 1988; Dissler et al., 1988; Doré et al., 1988; Chantraine et al., 1994; Butaeye et al., 2001; Le Gall et al., 2021), but the importance of the latter in the finite structural pattern is difficult to estimate because of major Variscan imprint in the study area. Emphasis is put below on the Late/Post-Variscan events extensively expressed in the northern offshore part of the CP area (Fig. 5).

The oldest structures reported here are a conjugate pattern of N40°E (sinistral) and N160°E (dextral) strike-slip faults (Figs. 10c, d) developed in the pre-Mesozoic basement to the south in response to a N-S shortening (Dissler and Gresselin, 1988; Doré et al., 1988; Vignerresse, 1988; Dupret et al., 1990). At that stage, strain preferentially focused along a number of N160°E faults, i.e. the Moncaneval and LHOF structures (Fig. 11). They are parts of a tardi/post-orogenic fault network widely distributed over most of the NW European Variscan belt and which will be later reactivated at various periods (Jurassic, Eocene and Oligocene to Neogene; Bois et al., 1990a, 1990b; Bonnet et al., 2000). The LHOF structure may belong to the NW/SE-oriented Sticklepath-Lustleigh (Holloway and Chadwick, 1986) fault system and its associated Cotentin Start-Point ridge which both extend further NW and mark the junction between the NE-SW structural pattern in the Western Approaches and the EW-oriented structures in the Central Channel basin to the NE (Fig. 1) (Lake and Karner, 1987).

The role of the basement structural configuration on the earlier development of the Meso-Cenozoic basins likely applies to the N100°E fault system (LHDF1/LHDF2) cutting through the Jurassic to Eocene series to the north. The interpretation of the proto-LHDF1 structure as a northerly-facing extensional fault controlling an Upper Jurassic sedimentary depocenter in its northern hangingwall block (Figs. 5, 7, 11) fits with the rifting event initiated during the Permo-Triassic in the nearby English Channel basins (Bois et al., 1990a, 1990b; Chadwick and Evans, 1995; Faure, 1995; Lericolais, 1997; Ballèvre et al., 2009; Le Roy et al., 2011; Bessin, 2014) in relation with early stages of the Pangea breakup that will later lead to the opening of the Atlantic Ocean (Chadwick, 1986). The parallelism of the LHDF1/LHDF2 fault network with Cadomian/Variscan onshore thrust structures (Fig. 2a) suggests its inherited origin. Additional support for this interpretation is supplied by the map trace of the LHDF1 structure which merges westwards into the N70°E Alderney-Ushant fault zone (AUFZ in Figs. 1, 2a), commonly regarded as a synrift structure rooting at depth along reactivated Variscan thrusts (Ziegler, 1987b; Beucler et al., 2021 and references therein).

Middle Jurassic/Lower Cretaceous deposits are apparently not present in the NW Cotentin offshore area so that structural events (uplift and possible basin inversion) experienced by adjacent basins during this time-period (Van Hoorn, 1987; Tucker and Arter, 1987; Lericolais, 1997) in relation with the opening of the Biscay bay (Roberts et al., 1981), are not recorded in the study area.

Cretaceous (chalk) and Eocene (carbonates) series in the CP offshore area are currently mostly confined in a southern fault-bounded 'block' (Fig. 11). However, their initial depositional distribution was probably much wider, as argued: (i) locally by the presence of Cretaceous series west of the tip point of the LHOF and (ii) at a larger scale by the widespread extent of these deposits in nearby English Channel basins (Ziegler, 1987a). On the EMECHAT seismic lines (EM031 and EM046, Figs. 7a, b), the Upper Cretaceous sequences are apparently conformably overlain by Eocene series. That suggests, at first approximation, that the mild inversion movements which initiated during Late Paleocene and early Eocene (Ypresian) in the Western Approaches basins (Bouysse et al., 1975; Ziegler, 1987b; Thinon et al., 2009; Le Roy et al., 2011; Bessin, 2014) did not affect the NW offshore CP area. This inhomogeneously distributed strain may result from the specific location of the CP area on the SE shoulder of the main axial depositional trough (Fig. 1) which temporarily escaped inversion processes because of the rigid mechanical behavior of the shallow basement. One additional controlling factor for the lack of Early Cenozoic inversion in the CP area could be

the decrease of strain intensity southwards, in a similar way as applied by Ziegler (1987b) about the little affected Armorican shelf south of the main Western Approaches basins (Fig. 1).

The single and regional-scale contractional event undergone by the CP shelf margin principally expressed by upright folding in the Jurassic series, synchronously to dextral wrenching along the LHDF1 and LHDF2 network and associated large wavelength folding in the fault-bounded Upper Cretaceous series and Eocene deposits (Figs. 5, 7, 11). These deformations typically relate to a transpressional setting recording a NW-SE shortening, prior to the deposition of unconformable fluvial sequences, inferred to be Plio-Quaternary in age (Fig. 11). This main phase of basin inversion correlates with the Oligo-Miocene compressional events experienced by most Celtic Sea and English Channel basins (Ziegler, 1981; Vandycke and Bergerat, 2001; Vandycke, 2002; Le Roy et al., 2011) in response to the combined effects of the Alpine and Pyrenean collisions (Sibuet et al., 1985). At that stage, the regional NW-SE fault network, including the Sticklepath-Lusleigh fault system, recorded wrench tectonics (Barr et al., 1981; Holloway and Chadwick, 1986; Lake and Karner, 1987). Therefore, it cannot be excluded that the vertical displacement recorded by the LHOF in post-Eocene times occurred during this regional strike-slip event. Another expression of the post-Eocene inversion in the southern part of the CP shelf margin could be the map-scale virgation undergone by the Upper Cretaceous/Eocene sequences under the buttress effect of the Variscan basement edge to the south (Figs. 5, 11a).

With respect to the monophasic tectonic scenario envisaged above, one remaining question concerns the contrasted tectonic styles between the folded Jurassic series (north of LHDF1) and the much less strained Cretaceous and Eocene series (mainly south of LHDF2). Three distinct (or complementary) mechanisms can be proposed: (i) a progressive decrease of strain intensity southwards (as already mentioned above about the lack of Paleogene deformation), (ii) a strain partitioning accommodated by the LHDF1/LHDF2 transverse fault system, and (iii) a contrasted behavior of the two mechanically distinct series during the deformation in relation with a differential coupling with the relatively shallow basement at depth (Upper Cretaceous directly overlying basement to the south).

The last geological event recorded in the study area is the dense pattern of deep incisions dissecting the Meso-Cenozoic strained cover, and more especially the Upper Cretaceous-Eocene series to the south, close to fault-bounded granitic basement terrains (Figs. 5, 7, 11). These erosional features and their subsequent Plio-Quaternary imbricated fluvial filling are extensively reported elsewhere in the English Channel (Lericolais et al., 2003; Benabdellouahed et al., 2014; Paquet et al., 2023). According to these authors, these processes took place during transgression/regression events related to glacio-eustatic cycles, when the sea-level was nearly 120 m lower than present-day. The dense pattern of erosional paleo-channels in the study area likely developed in direct connection with the English Channel river (Antoine et al., 2003; Lericolais et al., 2003; Paquet et al., 2023). In this regional context, the LHD constitutes the most prominent erosional channel. Its arcuate map trace, sub-parallel to the Upper Cretaceous/Eocene strata pattern, is seen to follow the northern edge of the granitic uplifted blocks (Auderville) to the SW, while abutting westwards against the easterly-facing LHOF scarp (Figs. 5, 7c, 11). Its eastern course tends to parallel the traces of LHDF1 and LHDF2, while the seismic sections suggest that the contact between Plio-Quaternary pack and basement is abrupt, rather steep, running along the map-trace of the LHOF. All this could mean that Plio-Quaternary tectonics could have played a role in the region. Its Plio-Quaternary fluvial infilling is in turn eroded as a consequence of high-energy tidal flows in the Alderney Race (Figs. 5, 7).

Our results also supply new insights about geohazard issues in the CP area. Among the identified fault network, two major steeply-dipping structures deserve special attention: the N160°E LHOF and the N100°E LHDF1. These faults are both inherited and long-lived structures which have been alternatively reactivated during the extensional and

contractional phases experienced by the CP area sensu lato in Meso-Cenozoic times (Fig. 11). Due to their post-Eocene deformation records, they still both remain good potential candidates for permanent seismic activity under the present-day NW-SE compressional stress-field (Delouis et al., 1993; Lagarde et al., 2000, 2003; Beucler et al., 2021). Even if displacements have occurred during Plio-Quaternary times, their inferred low-amplitude (meter-scale) makes them difficult to be detected with the seismic reflection techniques used in this study (Fig. 7).

6. Conclusions

The Cotentin area sensu lato, in the northwesternmost part of the Armorican massif (NW France), recorded a > 2 Ga-lasted geological history spanning in times from Archaean up to Recent. The resulting polyphase structural evolution encompasses extensional/basinal events which alternated with major compressional events (Cadomian/Variscan orogens) and ending with recent basin inversion processes during Late Tertiary. This paper, based on newly-acquired offshore geophysical dataset, aims to address the yet poorly-known structural evolution of the offshore Meso-Cenozoic cover west of the CP. When combined to the structural pattern of the onshore pre-Mesozoic substratum, our results lead us to establish an accurate spatio-temporal framework of post-Variscan structural events in part of the southern shelf margin of the Central English Channel. The main new insights of our work are as follow:

- The conjugate strike-slip fault pattern (N160°E dextral and N40–50°E sinistral) cutting through the pre-Mesozoic basement to the south is regarded as Late Variscan (Kerforne type) brittle structures which locally nucleated along earlier Variscan ductile shear zones (Moncaneval fault) and were later the locus of strain (LHOF).
- The N100°E-oriented La Hague Deep fault (LHDF1) which currently bounds a package of Upper Jurassic carbonate series to the north likely initiated as a northerly-facing extensional bounding fault during the major rifting event experienced by most of English Channel basins in Trias-Lower Cretaceous times. Its inherited origin, possibly along a reactivated Archaean and/or Cadomian thrust, is envisaged and fits with its connection westwards with the major N70°E Alderney-Ushant bounding fault also commonly regarded as reactivating preexisting Variscan discontinuities.
- The relatively thin Upper Cretaceous offshore sequences escaped the earliest effects of the Cenozoic compression which conversely affected parts of the English Channel basins in Paleogene times. The first evidence of basin inversion in our study area occurred later, in post-Eocene times, but prior to the deposition of recent (probably Plio-Quaternary) fluvio-glacial sediments. The inversion process principally expressed by local folding of the Jurassic series, coeval to dextral strike-slip movement along the reactivated LHDF1 structure and a satellite fault structure (LHDF2) to the south. At that stage, the LHOF structure might have recorded oblique displacement combining dextral wrenching and a vertical component.
- The Jurassic-Eocene strained terrains are deeply incised and unconformably overlain by Plio-Quaternary fluvio-glacial deposits. One of these recent incisions, i.e. the La Hague Deep, displays a prominent and arcuate bathymetric trace on the offshore DEM, following the Cadomian/Variscan structural grain in the underlying basement around the La Hague cape.
- The results above show that the NW offshore part of the CP area displays distinct stratigraphic and tectonic features with respect to adjacent Meso-Cenozoic English Channel basins. These specific features concern the relatively limited thickness of the Jurassic-Eocene sedimentary successions, as well as the localized distribution and moderate intensity of strain during basin inversion. All these stratigraphic and tectonic attributes likely relate to the strong influence of the shallow and rigid Paleozoic basement during the long-lasted

structural development of the elevated southern shelf margin of the Central English Channel.

- From a geohazard point of view, the proposed tectonic scheme supplies new constraints for a seismotectonic revised framework in the CP area. Some of the regional-scale faults investigated in this work, such as the LHOF and the LHDF1 and LHDF2 structures, should be explored in more details to characterize their recent tectonic activity and potential consideration in seismic hazard analyses.

CRedit authorship contribution statement

Tassadit Kaci: Writing – review & editing, Writing – original draft, Visualization, Software, Resources, Methodology, Investigation, Formal analysis. **Bernard Le Gall:** Writing – review & editing, Writing – original draft, Investigation, Formal analysis, Conceptualization. **Anne Dupret:** Writing – review & editing, Writing – original draft, Supervision, Project administration, Methodology, Investigation, Funding acquisition, Formal analysis, Conceptualization. **David Graindorge:** Writing – review & editing, Writing – original draft, Software, Methodology, Investigation, Formal analysis, Conceptualization. **Stephane Baize:** Writing – review & editing, Validation, Investigation, Formal analysis. **Yann Méar:** Supervision, Methodology, Investigation, Funding acquisition, Formal analysis, Data curation.

Declaration of competing interest

The authors declare that they have no known competing financial interests or personal relationships that could have appeared to influence the work reported in this paper.

Data availability

Bathymetry raw data are available on <https://data.shom.fr/>, IGN Altimetry data (RGE Alti) on <https://geoservices.ign.fr/>, LiDAR elevation data (Litto3D) on <https://rolnhdf.fr> and the submarine cored and dredged rocks on the BRGM marine database (<https://infoterre.brgm.fr/page/geoservices-ogc>). Additional coastal marine data obtained using french oceanographic fleet operated by IFREMER may be available following these direct links: BATHAGUE 2008 cruise: doi: [10.17600/8120080](https://doi.org/10.17600/8120080), BATHAGUE2010 cruise: doi: [10.17600/10120060](https://doi.org/10.17600/10120060), COCOTEC 19 cruise: doi: [10.17600/18000965](https://doi.org/10.17600/18000965) and EMECHAT cruise: doi: [10.17600/18002075](https://doi.org/10.17600/18002075).

Acknowledgments

This work is part of a Ph.D. thesis (T.K.). It received a grant awarded by the Normandy Region and was supported by the Tellus Programm of CNRS/INSU (COCOTIER project 2020) (A.D.). The COCOTEC-2019 (A. D.) and the EMECHAT-2022 (D.G.) cruises were operated on the IFREMER/FOF R/V Haliotis and the IFREMER/FOF R/V Côtes de la Manche, respectively. We would thank the Comité National Flotte Côtière (CNFC) and Genavir crews for their work, as well as Christophe Prunier and Emmanuel Poizot for their technical input onboard, Pauline Dupont for seismic support during the EMECHAT cruise and Johann Brochon for the first processing sequence of EMECHAT seismic lines and Juliette Thomas for the help during the interpretation and drawing of the three seismic profiles. We thank also Regis Gallon for the Unmanned Aerial Vehicle survey in the Moncaneval Bay. We greatly appreciate the constructive remarks and suggestions from the three anonymous reviewers and from the editor-in-chief: Michele Rebesco.

References

- Antoine, P., Coutard, J.-P., Gibbard, P., Hallegouet, B., Lautridou, J.-P., Ozouf, J.-C., 2003. The Pleistocene rivers of the English Channel region. *J. Quat. Sci.* 18, 227–243. <https://doi.org/10.1002/jqs.762>.

- Aubry, J., 1982. Formations permienues et triasiques du bassin de Carentan. Ph.D. thesis. Caen university, p. 285.
- Auvray, B., Charlot, R., Vidal, P., 1979. Données nouvelles sur le protérozoïque inférieur du domaine nord-armoricain (France): age et signification. *Can. J. Earth Sci.* 17, 532–538. <https://doi.org/10.1139/e80-050>.
- Avedik, F., 1975. The seismic structure of the Western Approaches and the South Armorian continental shelf and its geological interpretation. In: Woodland, A.W. (Ed.), *Petroleum and the continental shelf of North West Europe*. Applied Science Publishers, Barking, pp. 29–43.
- Bailly du Bois, P., 2010. BATHAGUE 2010 cruise. Haliotis R/V. <https://doi.org/10.17600/10120060>.
- Bailly du Bois, P., Dumas, F., Morillon, M., Furgerot, L., Voiseux, C., Poizot, E., Méar, Y., Bennis, A.-C., 2020. The Alderney Race: general hydrodynamic and particular features. *Philos. Trans. R. Soc.* 378, 22.
- Baize, S., 1998. Tectonique, eustaticisme et climat dans un système géomorphologique côtier. Le nord-ouest de la France au plio-pléistocène : exemple du Cotentin (Normandie). Ph.D. thesis. Caen university, p. 289.
- Baize, S., Lagarde, J.-L., Laville, E., Dugue, O., 1998. Géomorphologie d'un plateau littoral (Cotentin-Normandie): enregistrements des signaux tectoniques et climatiques. *Bull. Soc. Géol. France* 169, 851–866.
- Ballèvre, M., Bosse, V., Ducassou, C., Pitra, P., 2009. Palaeozoic history of the Armorican Massif: Models for the tectonic evolution of the suture zones. *Compt. Rendus Geosci.* 341, 174–201. <https://doi.org/10.1016/j.crte.2008.11.009>.
- Ballèvre, M., Bosse, V., Dabard, M.P., Ducassou, C., Fourcade, S., Paquette, J.-L., Peucat, J.-J., Pitra, P., 2013. Histoire Géologique du massif Armoricaire: Actualité de la recherche. *Bull. Soc. Géol. Minéral. Bretagne* 500, 5–96.
- Barr, K., Colter, V., Young, R., 1981. The geology of the Cardigan Bay-St. George's Channel Basin. In: Illing, L., Hobson, G. (Eds.), *Petroleum Geology of the Continental Shelf of North-West Europe*. Institute of Petroleum, Lond, pp. 432–443.
- Benabdellouahed, M., Dugué, O., Tessier, B., Thion, I., Guennoc, P., Bourdillon, C., 2014. Nouvelle cartographie du substratum de la baie de Seine et synthèse géologique terre-mer : apports de nouvelles données sismiques et biostratigraphiques. *Géol. Fr.* 1, 21–45.
- Bessin, P., 2014. Evolution géomorphologique du Massif armoricain depuis 200 Ma : approche Terre-Mer. Ph.D. thesis, Rennes 1 University, 377.
- Bessin, P., Guillocheau, F., Robin, C., Schroëtter, J.-M., Bauer, H., 2015. Planation surfaces of the Armorican Massif (western France): Denudation chronology of a Mesozoic land surface twice exhumed in response to relative crustal movements between Iberia and Eurasia. *Geomorphology* 233, 75–91. <https://doi.org/10.1016/j.geomorph.2014.09.026>.
- Bessin, P., Guillocheau, F., Robin, C., Braun, J., Bauer, H., Schroëtter, J.-M., 2017. Quantification of vertical movement of low elevation topography combining a new compilation of global sea-level curves and scattered marine deposits (Armorican Massif, western France). *Earth Planet. Sci. Lett.* 470, 25–36. <https://doi.org/10.1016/j.epsl.2017.04.018>.
- Beucler, É., Bonnin, M., Hourcade, C., Van Vliet-Lanoë, B., Perrin, C., Provost, L., Mocquet, A., Battaglia, J., Geoffroy, L., Steer, P., Le Gall, B., Douchain, J.-M., Fligiel, D., Gernigon, P., Delouis, B., Perrot, J., Mazzotti, S., Mazet-Roux, G., Lambotte, S., Grunberg, M., Vergne, J., Clément, C., Calais, É., Deverchère, J., Longuevergne, L., Duperret, A., Roques, C., Kaci, T., Authemayou, C., 2021. Characteristics and possible origins of the seismicity in northwestern France. *Comp. Rendus. Géosci.* 353, 53–77. <https://doi.org/10.5802/crgeos.86>.
- Bevan, T.G., Hancock, P.L., 1986. A late Cenozoic regional mesofracture system in southern England and northern France. *J. Geol. Soc.* 143, 355–362.
- Bitri, A., Brun, J.-P., Truffert, C., Guennoc, P., 2001. Deep seismic imaging of the Cadomian thrust wedge of Northern Brittany. *Tectonophysics* 331, 65–80. [https://doi.org/10.1016/S0040-1951\(00\)00236-5](https://doi.org/10.1016/S0040-1951(00)00236-5).
- Bois, C., Lefort, J.-P., Le Gall, B., Sibuet, J.-C., Gariel, O., Pinet, B., Cazes, M., 1990a. Traces of Caledonian and Proterozoic crustal features in deep seismic profiles recorded between France and the British Isles. *Tectonophysics* 185, 21–36.
- Bois, C., Lefort, J.-P., Le Gall, B., Sibuet, J.-C., Gariel, O., Pinet, B., Cazes, M., 1990b. Superimposed Variscan, Caledonian and Proterozoic features inferred from deep seismic profiles recorded between southern Ireland, southwestern Britain and western France. *Tectonophysics* 177, 15–37. [https://doi.org/10.1016/0040-1951\(90\)90272-A](https://doi.org/10.1016/0040-1951(90)90272-A).
- Bois, C., Cazes, M., Gariel, O., Lefort, J.-P., Le Gall, B., Pinet, B., Sibuet, J.-C., 1991. Principaux apports scientifiques des campagnes SWAT et WAM à la géologie de la Mer Celtique, de la Manche et de la marge atlantique. In: *Mémoires de La Société Géologique de France (1833)*, pp. 185–217.
- Bonnet, S., Guillocheau, F., Brun, J.-P., Van Den Driessche, J., 2000. Large-scale relief development related to Quaternary tectonic uplift of a Proterozoic-Paleozoic basement: The Armorican Massif, NW France. *J. Geophys. Res. Solid Earth* 105, 19273–19288.
- Bouysse, P., Horn, R., Lefort, J.-P., Le Lann, F., 1975. Tectonique et structures post-paléozoïques en Manche occidentale. *Philos. Trans. Royal Soc. London. A* 279, 41–54.
- Butaeye, D., Laville, E., Le Gall, J., 2001. Géométrie et cinématique des chevauchements variés du Nord-Est du Massif armoricain (France). *C. R. Acad. Sci. Ser. II A Earth Planet. Sci.* 332, 283–289. [https://doi.org/10.1016/S1251-8050\(01\)01542-7](https://doi.org/10.1016/S1251-8050(01)01542-7).
- Cara, M., Cansi, Y., Schlupp, A., Arroucau, P., Béthoux, N., Beucler, E., Bruno, S., Calvet, M., Chevrot, S., Deboissy, A., Delouis, B., Denieul, M., DESchamps, A., Doubre, C., Fréchet, J., Godey, S., Golle, O., Grunberg, M., Guilbert, J., Haugmard, M., Jenatton, L., Lambotte, S., Leobal, D., Maron, C., Mendel, V., Merrer, S., Macquet, M., Mignan, A., Mocquet, A., Nicolas, M., Perrot, J., Potin, B., Sanchez, O., Sautoire, J.-P., Sébe, O., Sylvander, M., Thouvenot, F., Van Der Woerd, J., Van Der Woerd, K., 2015. SI-Hex: a new catalogue of instrumental seismicity for metropolitan France. *Bulletin de la Société Géologique de France* 186 (1), 3–19.
- Chadwick, R.A., 1986. Extension tectonics in the Wessex Basin, southern England. *J. Geol. Soc.* 143, 465–488.
- Chadwick, R.A., 1993. Aspects of basin inversion in southern Britain. *J. Geol. Soc.* 150, 311–322.
- Chadwick, R.A., Evans, D.J., 1995. The timing and direction of Permo-Triassic extension in southern Britain. *Geol. Soc. Spec. Publ.* 91, 161–192. <https://doi.org/10.1144/GSL.SP.1995.091.01.09>.
- Chantraine, J., Rolet, J., Santallier, D.S., Piqué, A. (Eds.), 1994. *Pre-Mesozoic Geology in France and Related Areas*. Springer, Berlin Heidelberg. <https://doi.org/10.1007/978-3-642-84915-2>, 514.
- Chantraine, J., Egal, E., Thiéblemont, D., Le Goff, E., Guerot, C., Ballèvre, M., Guennoc, P., 2001. The Cadomian active margin (North Armorican Massif, France): a segment of the North Atlantic Panafrikan belt. *Tectonophysics* 331, 1–18. [https://doi.org/10.1016/S0040-1951\(00\)00233-X](https://doi.org/10.1016/S0040-1951(00)00233-X).
- Chantraine, J., Autran, A., Cavelier, C., 2003. Carte géologique de la France (version numérique) à l'échelle du millionième. BRGM, Orléans.
- Coutard, S., Lautridou, J., Rhodes, E., Clet, M., 2006. Tectonic, eustatic and climatic significance of raised beaches of Val de Saire, Cotentin, Normandy, France. *Quat. Sci. Rev.* 25, 595–611. <https://doi.org/10.1016/j.quascirev.2005.02.003>.
- Deconinck, J.F., Baudin, F., 2008. Kimmeridgian and Tithonian sedimentary deposits of the North-Western part of the Paris Basin (Normandy and Boulonnais). *Ann. Soc. Géol. Nord* 15, 77–90.
- Delouis, B., Haessier, H., Cisternas, A., Rivera, L., 1993. Stress tensor determination in France and neighbouring regions. *Tectonophysics* 221, 413–438.
- Dissler, E., 1987. Evolution géodynamique cadomienne du Nord-Cotentin (Massif armoricain). Ph.D. thesis. Caen university, p. 255.
- Dissler, E., Gresselin, F., 1988. The North Cotentin shear-zone (Normandy-France): Variscan mobilization of the Cadomian basement and its Palaeozoic cover. *Geol. J.* 23, 191–204.
- Dissler, E., Doré, F., Dupret, L., Gresselin, F., Gall, J.L., 1988. L'évolution géodynamique cadomienne du Nord-Est du Massif armoricain. *Bull. Soc. Géol. France* IV 801–814. <https://doi.org/10.2113/gssgfbull.IV.5.801>.
- Doré, F., Dupret, L., Lautridou, J.P., Hommeril, P., 1988. Notice explicative de la carte géologique de la France à (1/50 000), feuille Granville (172). BRGM, Orléans, p. 54.
- Dugué, O., Lautridou, J.-P., Quesnel, F., Clet, M., Poupinet, N., Bourdillon, C., 2009. Evolution sédimentaire cénozoïque (Paléocène à Pléistocène inférieur) de la Normandie. *Quaternaire. Rev. Assoc. Française pour l'Etude du Quat.* 20, 275–303.
- Duperret, A., 2019. COCOTEC 19 cruise. In: Haliotis R/V. <https://doi.org/10.17600/18000965>.
- Duperret, A., Vandycke, S., Mortimore, R.N., Genter, A., 2012. How plate tectonics is recorded in chalk deposits along the eastern English Channel in Normandy (France) and Sussex (UK). *Tectonophysics* 581, 163–181.
- Dupret, L., Dissler, E., Doré, F., Gresselin, F., Le Gall, J., 1990. Cadomian geodynamic evolution of the northeastern Armorican Massif (Normandy and Maine). *Geol. Soc. Lond., Spec. Publ.* 51, 115–131. <https://doi.org/10.1144/GSL.SP.1990.051.01.08>.
- Evans, C.D.R., Hillis, R.R., Gatliff, R.W., Day, G.A., Edwards, J.W.F., 1990. The geology of the western English Channel and its western approaches. HMSO, London, United Kingdom Offshore Regional Report for the British Geological Survey.
- Faure, M., 1995. Late orogenic carboniferous extensions in the Variscan French Massif Central. *Tectonics* 14, 132–153. <https://doi.org/10.1029/94TC02021>.
- Fourniguet, J., 1987. Géodynamique actuelle dans le Nord et le Nord-Est de la France. *Mémoire du BRGM (Paris)* 127, 173.
- Furgerot, L., Poprawski, Y., Violet, M., Poizot, E., Bailly du Bois, P., Morillon, M., Méar, Y., 2019. High-resolution bathymetry of the Alderney Race and its geological and sedimentological description (Raz Blanchard, northwest France). *J. Maps* 15, 708–718. <https://doi.org/10.1080/17445647.2019.1657510>.
- Graindor, M.J., 1998. Notice explicative de la carte géologique de la France à (1/50 000), feuille de Cherbourg (72), 6. BRGM, Orléans.
- Graindorge, D., 2022. EMECHAT cruise. R/V Côtes De La Manche. <https://doi.org/10.17600/18002075>.
- Gresselin, F., 1990. Evolution varisque du Massif armoricain oriental: insertion dans une transversale ouest-européenne. Ph.D. thesis. Caen university, p. 335.
- Guillocheau, F., Robin, C., Allemand, P., Bourquin, S., Brault, N., Dromart, G., Friedenberg, R., Garcia, J.-P., Gaulier, J.-M., Gaumet, F., Grosdoy, B., Hanot, F., Le Strat, P., Mettraux, M., Nalpas, T., Prijac, C., Rigollet, C., Serrano, G., Grandjean, G., 2000. Meso-Cenozoic geodynamic evolution of the Paris Basin : 3D stratigraphic constraints. *Geodin. Acta* 13, 189–246.
- Hamblin, R.J.O., Crosby, A., Balson, P.S., Jones, S.M., Chadwick, R.A., Penn, I.E., Arthur, M.J., 1992. The geology of the English Channel: United Kingdom Offshore Regional Report N°10. In: HMSO, London, United Kingdom Offshore Regional Report for the British Geological Survey.
- Holloway, S., Chadwick, R.A., 1986. The Sticklepath-Lustleigh fault zone: Tertiary sinistral reactivation of a Variscan dextral strike-slip fault. *J. Geol. Soc.* 143 (3), 447–452.
- Inglis, J.D., Samson, S.D., D'Lemos, R.S., Miller, B.V., 2005. Timing of Cadomian deformation and magmatism within La Hague, NW France. *J. Geol. Soc.* 162, 389–400. <https://doi.org/10.1144/0016-764904-006>.
- Jonin, M., Vidal, P., 1975. Etude géochronologique des granitoïdes de la Mancellia, Massif Armoricain, France. *Can. J. Earth Sci.* 12, 920–927.
- Klein, C., 1990. L'évolution géomorphologique de l'Europe hercynienne occidentale et centrale. In: *Mémoires et Documents de Géographie*, 177. Éditions du Centre National de la Recherche Scientifique, Paris.
- Lagarde, J.-L., Baize, S., Amorese, D., Delcaillau, B., Font, M., Volant, P., 2000. Active tectonics, seismicity and geomorphology with special reference to Normandy

- (France). *J. Quat. Sci. Pub. Quat. Res. Assoc.* 15, 745–758. <https://doi.org/10.1002/1099-1417>.
- Lagarde, J.L., Amorese, D., Font, M., Laville, E., Dugué, O., 2003. The structural evolution of the English Channel area. *J. Quat. Sci. Pub. Quat. Res. Assoc.* 18, 201–213. <https://doi.org/10.1002/jqs.744>.
- Lake, S.D., Karner, G.D., 1987. The structure and evolution of the Wessex Basin, southern England: an example of inversion tectonics. *Tectonophysics* 137, 347–378. [https://doi.org/10.1016/0040-1951\(87\)90328-3](https://doi.org/10.1016/0040-1951(87)90328-3).
- Lamarche, J., Bergerat, F., Mansy, J.-L., 1998. Déformations cassantes et plives dans le Jurassique du Boulonnais (France), influence lithostratigraphique et héritage paléozoïque. *C. R. Acad. Sci. Ser. IIA Earth Planet. Sci.* 57–63.
- Larsonneur, C., Horn, R., Auffret, J.-P., Hommeril, P., Moal, A., 1975. Géologie de la partie méridionale de la Manche centrale. *Philos. Trans. Royal Soc. London. A* 279, 145–153.
- Le Gall, B., Authemayou, C., Ehrhold, A., Paquette, J.-L., Bussien, D., Chazot, G., Aouizerat, A., Pastol, Y., 2014. LiDAR offshore structural mapping and U/Pb zircon/monazite dating of Variscan strain in the Leon metamorphic domain, NW Brittany. *Tectonophysics* 630, 236–250. <https://doi.org/10.1016/j.tecto.2014.05.026>.
- Le Gall, B., Authemayou, C., Graindorge, D., Duperré, A., Kaci, T., Ehrhold, A., Schmitt, T., 2021. Status of Basement Terranes in Orogens: Insights from the Cadomian Domain of the North Armorican Variscides, Western France. *Tectonics* 40. <https://doi.org/10.1029/2020TC006578>.
- Le Roy, P., Gracia-Garay, C., Guennoc, P., Bourillet, J.-F., Reynaud, J.-Y., Thinon, I., Kervevan, P., Paquet, F., Menier, D., Bulois, C., 2011. Cenozoic tectonics of the Western Approaches Channel basins and its control of local drainage systems. *Bull. Soc. Géol. France* 182, 451–463. <https://doi.org/10.2113/gssgfbull.182.5.451>.
- Lefort, J.-P., 1975. Le socle périarmorican : Etude géologique et géophysique du socle submergé à l'ouest de la France. PhD Thesis. Université de Rennes.
- Lericolais, G., 1997. Evolution du fleuve Manche depuis l'oligocène : stratigraphie et géomorphologie d'une plateforme continentale en régime périglaciaire. PhD Thesis. Université Bordeaux I, p. 265.
- Lericolais, G., Auffret, J.-P., Bourillet, J.-F., 2003. The Quaternary Channel River: seismic stratigraphy of its palaeo-valleys and deeps. *J. Quat. Sci.* 18, 245–260. <https://doi.org/10.1002/jqs.759>.
- Leutwein, F., Sonet, J., Zimmerman, J.-L., 1972. Dykes basiques du Massif Armorican septentrional, 1972. *Comptes Rendus Academie des Sciences* 275, 1327–1330.
- Martin, E., François, C., Paquette, J.-L., Capdevilla, R., Lejeune, A.-M., 2018. Petrogeochemistry and zircon U–Pb dating of the late Variscan Flamanville granodiorite and its Paleoproterozoic basement (Normandy, France). *Géol. Fr.* 1, 34–48.
- Masclé, A., Cazes, M., 1987. La couverture sédimentaire du Bassin parisien le long du profil ECORS-Nord de la France. *Rev. l'Institut Français du Pétrole* 42, 303–316.
- Mortimore, R., 2011. A chalk revolution: what have we done to the Chalk of England? *Proc. Geol. Assoc.* 122, 232–297. <https://doi.org/10.1016/j.pgeola.2010.09.001>.
- Paquet, F., Thinon, I., Dugué, O., Tessier, B., Benabdellouahed, M., Lasseur, E., Briais, J., Couéffé, R., Guennoc, P., Gaullier, V., 2023. *Mar. Pet. Geol.* 153 (2023), 106303 <https://doi.org/10.1016/j.marpetgeo.2023.106303>.
- Pareyn, C., L'Homer, A., 1989. Le bassin permien de Carentan. *Synthèse des bassins permien français. Mémoire du BRGM* 128, 288.
- Pedoja, Jara-Muñoz, J., De Gelder, G., Robertson, J., Meschis, M., Fernandez-Blanco, D., Nexas, M., Poprawski, Y., Dugué, O., Delcaillau, B., Bessin, P., Benabdellouahed, M., Authemayou, C., Husson, L., Regard, V., Menier, D., Pinel, B., 2018. Neogene-Quaternary slow coastal uplift of Western Europe through the perspective of sequences of strandlines from the Cotentin Peninsula (Normandy, France). *Geomorphology* 303, 338–356. <https://doi.org/10.1016/j.geomorph.2017.11.021>.
- Raimbault, C., Duperré, A., Le Gall, B., Authemayou, C., 2018. Structural inheritance and coastal geomorphology in SW Brittany, France: An onshore/offshore integrated approach. *Geomorphology* 306, 141–154. <https://doi.org/10.1016/j.geomorph.2018.01.018>.
- Roberts, D.G., Montadert, L., Charpal, D., 1981. Continental margin from the Porcupine Seabight to the Armorican marginal basin. In: Illing, L.V., Hobson, G.D. (Eds.), *Petroleum Geology of the Continental Shelf of Northwest Europe*. Heyden, London, pp. 455–473.
- Rolet, J., Gresselin, F., Jegouzo, P., Ledru, P., Wyns, R., 1994. Intracontinental hercynian events in the Armorican Massif. In: *Pre-Mesozoic Geology in France and Related Areas*. IGCP-Project 233. Springer, Berlin, Heidelberg. https://doi.org/10.1007/978-3-642-84915-2_20.
- Sibuet, J.-C., Mathis, B., Pastouret, L., Auzende, J.-M., Foucher, J.-P., Hunter, P., Guennoc, P., de Graciansky, P.-C., Montadert, L., Masson, D.G., 1985. 56. Morphology and Basement Structures of the Goban Spur Continental Margin (Northeastern Atlantic) and the Role of the Pyrenean Orogeny. Initial Reports of the Deep Sea Drilling Project 80 (Part VIII), 1153–1165.
- Stonley, R., 1992. Review of the Habitat of Petroleum in the Wessex Basin: Implications for Exploration. *Proceedings of the Usher Society* 8, 1–6.
- Thinon, I., Fidalgo-González, L., Réhault, J.-P., Olivet, J.-L., 2001. Déformations pyrénéennes dans le golfe de Gascogne. *C. R. Acad. Sci. Ser. IIA Earth Planet. Sci.* 332, 561–568. [https://doi.org/10.1016/S1251-8050\(01\)01576-2](https://doi.org/10.1016/S1251-8050(01)01576-2).
- Thinon, I., Menier, D., Guennoc, P., Proust, J.-N., 2009. Carte géologique de la France à 1/250 000: Marge continentale–Lorient Bretagne Sud Première édition. BRGM, Orléans.
- Tucker, R.M., Arter, G., 1987. The tectonic evolution of the North Celtic Sea and Cardigan Bay basins with special reference to basin inversion. *Tectonophysics* 137, 291–307.
- Van Hoorn, B., 1987. The south Celtic Sea/Bristol Channel Basin: origin, deformation and inversion history. *Tectonophysics* 137, 309–334.
- Van Vliet-Lanoë, B., Mansy, J.-L., Henriot, J.-P., Laurent, M., Vidier, J.-P., 2004. Une inversion tectonique cénozoïque par étapes : le Pas-de-Calais. *Bull. Soc. Géol. France* 175, 175–195. <https://doi.org/10.2113/175.2.175>.
- Vandycke, S., 2002. Palaeostress records in Cretaceous formations in NW Europe: extensional and strike-slip events in relationships with cretaceous-Tertiary inversion tectonics. *Tectonophysics* 357, 119–136.
- Vandycke, S., Bergerat, F., 2001. Brittle tectonic structures and palaeostress analysis in the Isle of Wight, Wessex basin, southern U.K. *J. Struct. Geol.* 23, 393–406. [https://doi.org/10.1016/S0191-8141\(00\)00125-5](https://doi.org/10.1016/S0191-8141(00)00125-5).
- Vignerresse, J.-L., 1988. La fracturation post-hercynienne du Massif armorican d'après les données géophysiques. *Géol. Fr.* 4, 3–10.
- Whittaker, A., 1985. Atlas of onshore sedimentary basins in England and Wales: post-Carboniferous tectonics and stratigraphy, 80. Kluwer Academic Publishers.
- Ziegler, P.A., 1981. Evolution of sedimentary basins in North-West Europe. In: Illing, L. V., Hobson, G.D. (Eds.), *Petroleum Geology of the Continental Shelf of North-West Europe*, pp. 3–39.
- Ziegler, P.A., 1987a. Celtic Sea-Western Approaches area: an overview. *Tectonophysics* 137, 285–289.
- Ziegler, P.A., 1987b. Evolution of the Western Approaches Trough. *Tectonophysics* 137, 341–346. [https://doi.org/10.1016/0040-1951\(87\)90327-1](https://doi.org/10.1016/0040-1951(87)90327-1).
- Ziegler, P.A., 1987c. Late Cretaceous and Cenozoic intra-plate compressional deformations in the Alpine foreland-a geodynamic model. In: Ziegler, P.A. (Ed.), *Compressional Intra-Plate Deformations in the Alpine Foreland*, *Tectonophysics*, 137, pp. 389–420.
- Ziegler, P., 1990. Geological atlas of western and central Europe, 239. *Shell International Petroleum, Mijdrecht*.
- Ziegler, A.M., Scotese, C., McKerrow, W., Johnson, M., Bambach, R., 1979. Paleozoic Paleogeography. *Annu. Rev. Earth Planet. Sci.* 7, 473–502. <https://doi.org/10.1146/annurev.ea.07.050179.002353>.
- Ziegler, P.A., Cloetingh, S., van Wees, J.-D., 1995. Dynamics of intra-plate compressional deformation: the Alpine foreland and other examples. *Tectonophysics* 7–59. [https://doi.org.proxy-bu2.u-bourgogne.fr/10.1016/0040-1951\(95\)00102-6](https://doi.org.proxy-bu2.u-bourgogne.fr/10.1016/0040-1951(95)00102-6).